

THE EFFECT OF WOBBLING MASS ON
KNEE JOINT FORCE ESTIMATES

THE CONTRIBUTION OF BELOW KNEE WOBBLING MASS
TO THE ESTIMATION OF VERTICAL KNEE JOINT REACTION FORCES
FOLLOWING IMPACT WITH THE GROUND.

By

DAVID MORGAN ANDREWS, B.P.E.

A Thesis

Submitted to the School of Graduate Studies

in Partial Fulfilment of the Requirements

for the Degree

Master of Science

McMaster University

(c) Copyright by David Morgan Andrews, July, 1992

MASTER OF SCIENCE (1992)
(Biomechanics)

McMASTER UNIVERSITY
Hamilton, Ontario

TITLE: The Contribution of Below Knee Wobbling Mass
to the Estimation of Vertical Knee Joint Reaction
Forces Following Impact With the Ground.

AUTHOR: David Morgan Andrews, B.P.E. (McMaster University)

SUPERVISOR: J.J. Dowling, Ph.D.

NUMBER OF PAGES: x, 87

ABSTRACT

In human impacts involving high peak accelerations, the wobbling mass (skin, muscle, fat, and connective tissue) of the body will accelerate independently of the rigid mass (bone). The purpose of this study was to quantify the effect that below knee wobbling mass has, if any, on the attenuation of peak forces transmitted through the leg to the knee joint, following impacts with the ground. Fifteen healthy subjects dropped vertically from heights of 5 and 10 cm, onto a force platform, with the ankle and knee joints of the support leg held rigidly. A uni-axial accelerometer was fixed, with skin bond cement, to the skin overlying the anterior upper tibia, and another to the posterior wobbling tissue of the support limb. Vertical ground reaction forces and accelerations were used in rigid only and rigid and wobbling link segment models of the leg, which resulted in estimates of vertical knee joint reaction forces (VKJRF). Mean peak VKJRFs resulting from rigid only calculations were $2.66 \pm .55$ x body weight (bw) and $3.53 \pm .68$ x bw, and from rigid and wobbling calculations were $2.64 \pm .55$ x bw and $3.52 \pm .68$ x bw, for the 5 and 10 cm heights, respectively. A two-way, repeated measures ANOVA revealed that there was no main effect for calculation method.

Validation of the subject results was attempted indirectly by comparing them to the actual forces (load cell)

at the knee of a manufactured model. The model was constructed in proportion to a human subject of mass 75 kg.

When the model was dropped from the same heights as the subjects, the mean peak VKJRFs ($22.9 \times bw$) greatly overestimated the actual load cell values ($8.2 \times bw$), and were unrealistic relative to subject values (approximately $3.0 \times bw$). Although mean peak VKJRFs were also overestimated when the wobbling mass accelerations were included, they were much closer to the actual values ($9.9 \times bw$ vs. $8.2 \times bw$).

ACKNOWLEDGEMENTS

The completion of this project was made possible by the assistance of the following persons: my Thesis Committee members Dr. James J. Dowling, Dr. Cindy Riach, Dr. Robert W. Norman, and Dr. Michael Pierrynowski; John Moroz, for his time and expert advice regarding the design of the mechanical model; Drake Andrews and John Stassen, for their timely contributions to the quick release assembly; Gaye Andrews, for her efforts in locating a source of the cement used for accelerometer fixation; and all the subjects, who volunteered their time and bodies to the cause, without complaint.

LIST OF FIGURES

1.	Schematic representation of a fourth order, two degree of freedom visco-elastic model of the human body	15
2a.	Diagram of experimental setup for subjects	25
2b.	Photograph of one subject hanging on the actual experimental apparatus	26
3a.	Schematic diagram of manufactured mechanical model	28
3b.	Photograph of the actual mechanical model	29
3c.	A schematic diagram of the rigid and wobbling mechanical model.....	30
4.	Photograph showing lower portion of the mechanical model including the wobbling mass portion, on the posterior aspect of the rigid leg; the pin guiding system; and the elastic band connections	31
5a.	A photograph showing the quick release apparatus, with electromagnet, used to suspend and then release the mechanical model	33
5b.	A photograph depicting the mechanical model suspended by the quick release apparatus	34
6.	A free body diagram of a rigid and wobbling leg in dynamic equilibrium.....	38
7.	Accelerometer mounting sites on the rigid and wobbling sections of the leg	41
8.	Rigid mass and wobbling mass acceleration curves (a) and (b), ground reaction force curve (c), and corresponding VKJRFs (d), for one trial of a typical subject	48
9.	Enlargements of the VKJRF curves shown in Figure 8d ...	51
10.	Linear envelope EMG from medial gastrocnemius (a), tibialis anterior (b), biceps femoris (c), and vastus lateralis (d), and the corresponding ground reaction force (e), for one subject	53

11. Rigid mass and wobbling mass acceleration curves (a) and (b), and corresponding ground reaction force curve (c), for a typical trial for the model 56

12. VKJRFs generated using only rigid acceleration (a); VKJRFs generated using rigid and wobbling accelerations (b); actual VKJRFs (c), for a typical trial for the model 61

LIST OF TABLES

1.	Actual and calculated ideal masses of rigid and wobbling components of the mechanical model	37
2.	Mean absolute rigid and wobbling mass acceleration results for all subjects (n=15)	47
3.	Mean absolute ground reaction force results for all subjects (n=15)	50
4.	Mean absolute subject VKJRF data	52
5.	Mean EMG results for two subjects landing from 10 cm	54
6.	Mean absolute rigid and wobbling mass acceleration results for the mechanical model	57
7.	Mean absolute ground reaction force results for the mechanical model	59
8.	Mean absolute model VKJRF results	60
9.	Mean "goodness of fit" results for actual (LCRy) and estimated (RRy and RWRy) VKJRFs	62

INTRODUCTION

The determination of the internal forces acting at joints in the human body is traditionally accomplished in biomechanics with the aid of link segment analyses. Inherent in these analyses is the assumption that all body segments are rigid bars of material held together by hinge connections at the joints. However, the soft tissues of the body can, and do, move independently relative to bone in certain human movements. This would indicate that the combined tissue mass of each body segment does not always behave as a bar of rigid material. One example of this to which we can all identify, is the wobbling of leg soft tissues seen during slow motion replay of a person running.

The application of any model whose fundamental assumptions do not meet a given situation, must be questioned. It follows then, that the movements of non-rigid body tissue (relative to bone) witnessed during impacts such as the single support phase of running, must be quantified in order to comment on the accuracy of rigid-only link segment models in these cases.

The practical importance of accurate kinetic information from link segment models, apart from those models used for strictly research purposes, can be seen in the following two examples.

In the world of competitive sport, elite athletes and coaches rely on many sources of information in order to improve performance. Biomechanical analyses of athletic performances are in common use today for this purpose. Visual feedback to the athlete regarding the kinematics of a personal performance may take the form of a stick figure representation of themselves, obtained from segment displacements captured on film. With the aid of link segment modelling, kinetic information can be derived from the kinematic information discussed above, using inverse dynamics calculations. The point to be made here is simply this; the better the predictive ability of the model, the better the representation of realistic human segmental interactions, and hence, the better the application potential to athletes and coaches, for performance evaluation and related purposes.

Predicted vertical joint reaction forces in the range of 1 to 3 times body weight (bw) have been found to be present in the knee joint during vertical impacts, such as walking (Morrison, 1970; Gilbert et al., 1984). Compressive knee joint forces in the range of $24 \times bw$ have also been reported following landing from a height of over 1 m (Smith, 1975). Repetitive, chronic exposure to external impact induced forces with magnitudes in the range of body weight, have been shown to contribute to knee joint injuries in rabbits (Radin et al.,

1973), in sheep (Radin et al., 1982), and in guinea pigs (Simon et al., 1972), and to a variety of musculoskeletal maladies in humans, including ankle and knee pain (Voloshin and Wosk, 1981), and back pain (Light et al., 1980; Voloshin and Wosk, 1981; Voloshin and Wosk, 1982). Microtrauma joint injuries such as articular cartilage degeneration, and trabecular microfractures, were seen in the loaded knee joints of the rabbits (Radin et al., 1973), and guinea pigs (Simon et al., 1972). Similar joint injuries have also been noted in human subjects (Radin et al., 1973).

To reduce the magnitude of these impact induced joint forces, and hence their likely contribution to joint injury, it is important in some cases that additional force attenuating materials be utilized, in the form of shoe soles and corrective orthotic devices (Light et al., 1980; Voloshin and Wosk, 1981; Nigg et al., 1988; Bordelon, 1989; Rome, 1990; Rome, 1991). The degree of damping required to attenuate high joint forces is dependent, to some degree, on the magnitude of the joint forces involved. Consider the case where the magnitude of the vertical joint reaction forces at the knee were overestimated, and hence force attenuating shoe orthotics were prescribed. The general rule would be to prescribe a less rigid orthotic (more damping) in order to better absorb or attenuate the perceived high joint forces (Bordelon, 1989; Rome, 1991). In this case, the prescription of the shoe

orthotic may not have been necessary (since the peak joint force was overestimated) and if used as prescribed, may in fact contribute to other time dependent injuries which could have initially been avoided.

The use of rigid link segment models in biomechanics is widespread, due in part to the relative simplicity of the calculations involved. But are we missing something by using these models, for simplicity's sake? To improve on the predictive ability of rigid link segment models in certain situations, it may be appropriate to challenge one of the underlying assumptions of these models; that the tissues of human segments can be adequately modelled as completely rigid in nature. It has been speculated that errors in ground reaction force (GRF) estimations, using an inverse dynamics approach, could be a result of adhering to this basic assumption (Sanders et al., 1991). Specifically, it was reported that during the first 20% of contact with the force platform, following initial impact, GRFs were overestimated. It was suggested that the overestimation of GRFs may have been a result of the rigid model's inability to explain the independent, high magnitude accelerations of the rigid and non-rigid masses likely to occur immediately following impact (Sanders et al., 1991). Gruber et al. (1987), also showed that the soft tissue or "wobbling mass" components (muscle, fat, skin and connective tissue) of the human body rotate and

translate independently of the rigid mass (bone), following impact with the ground.

The validity of using a rigid only link segment model for the trunk was investigated by McGill et al. (1989). It was found that when the rise times (RT) of applied forces to the trunk were less than 300 ms, a completely rigid model lead to inaccurate estimations of the peak forces transmitted through the segment due to the attenuation of the forces by the soft trunk tissues.

In agreement with the speculation made by Sanders et al. (1991), and the findings of McGill et al. (1989) and Gruber et al. (1987), it is suggested here that improved estimates of inter-segmental joint forces can be made if the composition of the body segments, making up the linked model, are changed to more realistically represent the anatomy of our own bodies. That is, to model the body segments as having both rigid and non-rigid tissue components.

The purposes of this study then, were as follows:

- (i) to determine whether below knee wobbling mass has a significant effect on attenuating peak forces which are transmitted through the leg to the knee joints of subjects following impact with the ground.

(ii) to validate subject results against actual vertical joint reaction forces measured at the knee joint of a manufactured mechanical model.

It was the hypothesis of this study that the omission of below knee wobbling mass would lead to overestimations of the actual vertical joint reaction forces at the knees of subjects.

REVIEW OF LITERATURE

The independent movement of rigid (bone) and non-rigid (muscle, skin, fat, connective tissue) components of human body segments, will depend on several factors including the degree to which the muscular component of the non-rigid tissue is neurally activated, the magnitude and method of force application to the body, and the relative quantities of rigid and non-rigid tissue comprising the body segments.

Muscle Activation

The degree to which the muscular component of the non-rigid tissue is neurally activated should be considered for several reasons. Firstly, it is hypothesized here that the more the muscular component is activated (increasing the muscular stiffness), the more rigid the entire segment becomes, and as a result, the smaller the effect due to wobbling mass. And secondly, an activated muscular component will contribute to bone-on-bone forces (BOB) at the joint(s) crossed by those muscles comprising the muscular component of the wobbling tissue.

Regarding the first case above, Cavagna (1970) showed that when subjects landed from a height onto the balls of the feet without bending the knees, and with calf muscles in sustained contraction (stiff), the elastic stiffness of the oscillating tissues of the leg increased with increased load.

From the stiffnesses calculated at each of the loads, Cavagna (1970) was able to show that the response trend of the elastic structures on which the body bounced following impact was similar to that of the series elastic component of isolated muscle. In other words, the stiffness of the leg musculature is reflected in the oscillation of the body due to the inherent elastic structures. Contrary to this finding, McGill et al., (1989), found that altering the stiffness of the trunk musculature by varying the degree of muscle activation did not notably change the attenuating nature of the trunk to applied forces.

In the latter case above, BOB forces at a joint were defined as the result of muscular forces and joint reaction forces at that joint (Galea and Norman, 1985). Using this definition, Galea and Norman (1985) calculated BOB forces at the ankle joint of three ballet dancers during rapid foot movements involving springing from flat feet onto the points of the toes. The muscle activations of six muscles crossing the ankle joint were monitored using electromyography. It was found, in some cases, that BOB forces were as high as $10 \times bw$. When compared to the peak ankle joint reaction forces alone, it indicated that muscle co-contractions contributed markedly to the overall load seen at the joint articulations. It was concluded then, that the use of joint reaction forces alone would have lead to an underestimation of the force applied to

the articulating surfaces of the joint (Galea and Norman, 1985).

Body Composition Determination

In order to be able to explain the force attenuating contribution of the rigid and non-rigid or wobbling tissue of the segments of the body, it is necessary to determine the quantity of mass occupied by each tissue component. Despite the development of new technologically advanced, indirect methods used to determine human body composition, including dual-photon absorptiometry (DPA), magnetic resonance imaging (MRI), and electrical conductance (Lukaski, 1987; Brodie, 1988), cadaveric dissection remains the only direct method used to determine the mass of individual tissues of the body (Brodie, 1988). Although the determination of rigid and non-rigid body tissue mass using DPA, for example, is considered to be an accurate measure (Lukaski, 1987; Brodie, 1988; Galea et al., 1990), the proportion of rigid to non-rigid tissue mass for individual limb segments of living subjects, is not yet available in the literature. We must still rely then on past cadaveric studies for this information.

Several studies involving human cadaver dissection for purposes of determining the mass of body tissues, have been performed in the past (Dempster and Gaughran, 1967; Clarys et al., 1984; Clarys and Marfell-Jones, 1986a; Clarys and Marfell-Jones, 1986b). The determination of the component

tissue masses of individual segments of the body has also been done, although, the number of studies is limited. Dempster and Gaughran, (1967) reported skin and fascia, muscle, and bone tissue masses for the thigh, shank, foot, arm, forearm, hand, and shoulder as a percent of the total weight of the subject. A more recent study by Clarys and Marfell-Jones, (1986a) reported skin, adipose, muscle, and bone tissue masses for the thigh, leg, foot, hand, arm, and forearm segments in grams. The number of cadavers involved in this study was small (3 male and 3 female), and the mean age of the subjects was 66.8 years. Although old, each of the cadavers was embalmed, a technique which involves the re-introduction of fluid into the cadaver in order to restore the tissue circumference known to decrease as a result of tissue deterioration following death (Clarys and Marfell-Jones, 1986b). It is thought then, that tissue masses obtained in this manner closely reflect the tissue masses in living subjects.

The Notion of Wobbling Mass

The notion that link segment models should comprise some form of wobbling or non-rigid tissue mass in conjunction with the rigid mass, for the purpose of kinetic investigations of the human body in motion, was first noted in the literature by Gruber et al., (1987). The non-rigid or wobbling mass, as defined by Gruber et al., was comprised of skin, muscle, fat

and connective tissue and translated and rotated with respect to the rigid or long axis (bone) of the segment. The interaction between the rigid and wobbling mass sections was reported to be quasi-elastic and strongly damped in nature.

Attempting to validate the wobbling mass model, Gruber et al. (1987), compared the calculated motion of the wobbling mass sections of the lower extremity, to the motion as derived from high-speed filming of subjects landing from a vertical jump. The agreement between these two motions was reported to be excellent. Gruber et al. went on to say however, that the relative motions of the rigid and wobbling mass sections of the segments prevents accurate evaluation of the system even using high-speed filming. Also, data supporting the "excellent agreements", which were reported to occur, were not presented in the manuscript.

In order to test the validity of using a rigid only link segment model of the human trunk in loaded situations, McGill et al., (1989) manually applied loads to force transducers mounted either on the shoulders, at the hands, or on the crown of the heads of subjects, while in a seated position, on top of a force platform. Peak forces created by adding mass to the shoulders, by pulling up with the hands, or by striking the crown of the head with a hammer, were transmitted through the trunk and were measured as output by the force platform. McGill et al., (1989) indicated that for

applied forces with rise times of less than 20 ms (from the hammer), up to 40% of the applied peak force was reduced after travelling through the trunk. For rise times of between 30 ms and 300 ms, it was found that output forces were greater in magnitude than were the applied forces. The larger peak output forces were said to be a result of some of the trunk mass "rebounding" following impact. In short, there were alterations to the applied forces due to the movement of non-rigid tissue of the trunk segment. It was concluded that a rigid-only link segment model of the trunk was justified when the rise time of the applied forces was more than about 300 ms (McGill et al., 1989).

Visco-elastic Models

Visco-elastic models of the human body have also been proposed in order to describe the impact response of the body following vertical collisions with the ground. The resulting oscillatory response of the combined body mass to impacts, has been likened to that of mechanical systems comprised of elastic springs and viscous dampers (Walshaw, 1984). Oscillations of the non-rigid tissue mass of the human body will be in the direction of any external force imparted on it, and will be dependent on the elastic and viscous properties of which the body tissue, and connections between the body tissues are made. In the case of the human body, the amplitude and frequency response of the oscillating mass is

dependent on the inherent visco-elastic properties of and between the soft tissue (muscle, fat, skin, connective tissue), and the rigid tissue (bone).

The visco-elastic response of the human body to impacts with the ground after falling vertically from a height, has been investigated in the literature (Cavagna, 1970; Mizrahi and Susak, 1982a; Mizrahi and Susak, 1982b; Özgüven and Berme, 1988). Linear models built to represent the visco-elastic nature of the tissues of the body do so by separating the body into masses, springs (elastic components of each tissue type), and dampers (viscous friction between muscle and surrounding tissue, and within the tissues themselves). Mechanically speaking, the elastic tension across a spring is directly proportional, by a constant spring stiffness k , to the displacement y , of the spring. The viscous force across a damper is directly proportional, by a constant damping coefficient c , to the velocity \dot{y} , of the damper. In other words, the visco-elastic response of a mass m , to an external force F , can be described as in Equation [1], where \ddot{y} is the linear acceleration of mass m .

$$m \ddot{y} + c \dot{y} + k y = F \quad [1]$$

A form of Equation [1] was used by Cavagna (1970), to describe the elastic bounce of the human body following a

vertical impact with the ground. In this case, the mass of the system consisted of the total mass of the body. The oscillatory motion of this mass was determined by a single linear spring and damper. The stiffness and damping coefficient of the spring and damper system, were determined from the frequency of the body oscillations under load (Cavagna, 1970).

Dividing the total body mass into two separate units of mass (\underline{m}_2 above the hip joint, and \underline{m}_1 below) creates an interactive visco-elastic model of the body requiring two springs with stiffnesses \underline{k}_1 and \underline{k}_2 , and two dampers with damping coefficients \underline{c}_1 and \underline{c}_2 (Figure 1). Two degree of freedom models such as in Figure 1, give provision for the determination of the interactive motions of the individual masses involved, following some perturbation to the system. The equations which describe the motion of the oscillating masses \underline{m}_1 and \underline{m}_2 , are similar in form to Equation [1]. However, the relative motion of each mass is accounted for separately. Analysis of free body diagrams of the individual masses \underline{m}_1 and \underline{m}_2 , yields Equations [2] and [3] below (Mizrahi and Susak, 1982a; Özgüven and Berme, 1988).

$$m_1 \ddot{Y}_{M1} + (c_1 + c_2) \dot{Y}_{M1} + (k_1 + k_2) Y_{M1} - c_2 \dot{Y}_{M2} - k_2 Y_{M2} = F(t) \quad [2]$$

$$m_2 \ddot{Y}_{M2} + c_2 (\dot{Y}_{M2} - \dot{Y}_{M1}) + k_2 (Y_{M2} - Y_{M1}) = 0 \quad [3]$$

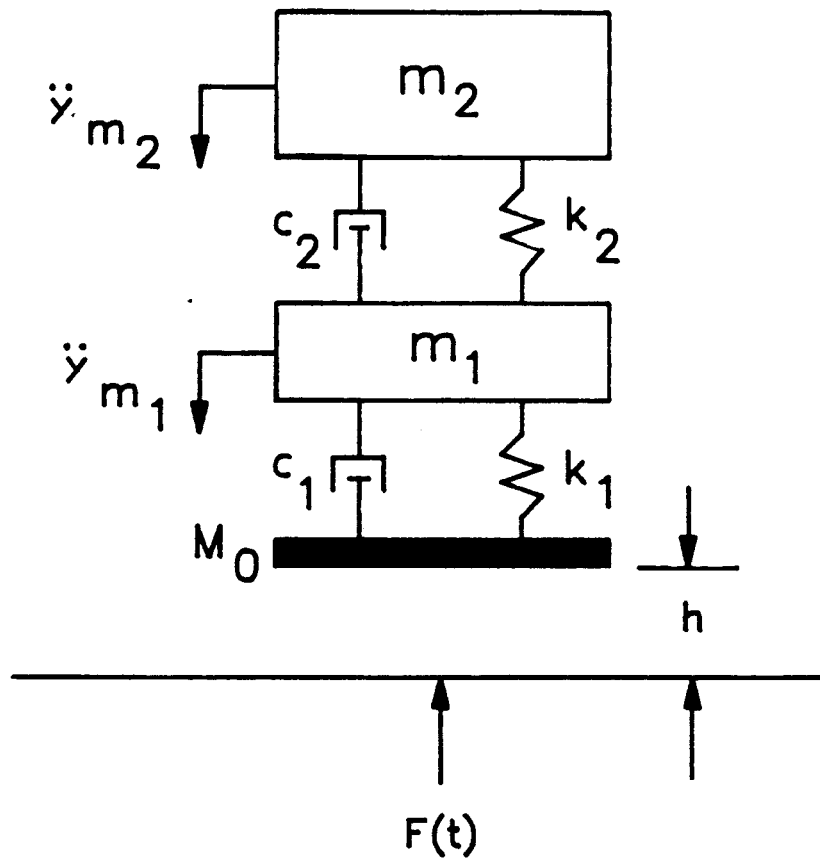


Figure 1: Schematic representation of a fourth order, two degree of freedom visco-elastic model of the human body. M_0 is a massless foot, h is the height dropped, $F(t)$ is the ground reaction force at landing, and \ddot{y}_{m_1} and \ddot{y}_{m_2} are the vertical linear accelerations of m_1 and m_2 respectively.

Consequent to vertical impacts of the lower extremities with the ground, are high peak ground reaction forces which are transmitted through the tissues of the supporting limb(s), to and through supporting joints, and into the rest of the body. The attenuation of these transmitted forces is important if damage to joints is to be avoided (Radin et al., 1973; Mizrahi and Susak, 1982a; Salathé et al., 1990). The contribution of natural shock absorbers such as bone, and articular joint cartilage, to the attenuation of transmitted forces through the body during impact, is enhanced by the deformation of the feet and their supporting tendons and ligaments (Salathé et al., 1990), as well as by controlled flexions at the ankle, knee and hip joints (Mizrahi and Susak, 1982b). To comment on the effect that the transmitted ground reaction forces have however, on the motion of the rigid and non-rigid tissue of the supporting limb(s), joint flexions during landing must be controlled. Mizrahi and Susak, (1982a) and Cavagna, (1970) attempted this by having subjects land from a height above the ground with legs locked at the knee and ankle. Without the aid of joint stabilizing devices, such as braces, to restrict joint movements in the sagittal plane, subjects having to land with stiff lower extremities may require practice in order to master the exercise without a loss of stability, and/or without tissue motion interference caused by contraction of antagonistic musculature (Cavagna,

1970).

Methodologies such as the ones described above, although effective in determining the oscillatory motion of the human body as a whole, do not attempt to determine the relative motions of the individual tissue components of body segments caused by the introduction of an external force. Attempts to do this were made in a study by Paul et al., (1978), in which the relative contribution of bone and soft tissues, to the force attenuating ability of the lower extremity of the rabbit, was described as a function of the frequency of the loads applied to the foot. Rabbits were constrained on a pivoting table such that their rear right legs hanged vertically downward. The ankle of each leg was splinted, leaving the lower extremity (leg and foot) as one rigid segment. External forces were imparted on the rabbit leg at the heel, at known frequencies. A force transducer was mounted in the knee joint of the restrained leg in order to measure the inter-joint forces resulting from the applied forces at the heel. Soft tissue components of the leg were surgically removed in sections enabling the determination of the force attenuating contribution of the soft tissue. Although the precise relative contributions of the rigid and soft tissue components of the rabbit leg could not be determined precisely in this study, it was reported that the

soft tissue components of the leg did contribute, to some degree, to the attenuation of the inflicted peak forces. It was also reported that the attenuation of peak forces by the bone and soft tissue was most effective at high frequencies (80% peak force attenuation at 60 Hz increasing to almost 100% at 360 Hz).

High frequency impulses of about 100 Hz were also reported by Munroe et al., (1975) for humans during heel strike of gait. This would indicate that the soft tissue components of the lower extremity have an effect on the attenuation of peak forces during human impacts with the ground.

Viscous Damping of Vibrating Systems

All matter is capable of vibration when perturbed by an external force. The type, amplitude, and frequency of the induced vibration depends on many factors including the magnitude of the applied external force, the mass of the system, and the viscous and elastic properties inherent in the system. For instance, the viscous damping in a vibrating mechanical system dissipates energy, which concomitantly reduces the efficiency of that system. To maintain the vibration more energy must be introduced to the system to compensate for the energy lost through viscous damping (Walshaw, 1984). In the human mechanical system, the non-rigid tissue attached to the rigid bone will oscillate when

the body is perturbed by an external force. The oscillations created will be damped due to the viscous properties of the musculoskeletal system, and therefore, energy will be lost.

For the reason mentioned above, it is important to be able to determine quantitatively, the amount of viscous damping present within a given mechanical system. The determination of the amount of damping present within an oscillating system (including the human system) can be made simply, by measuring the decrease in the amplitudes of two successive oscillations (Hatze, 1975; Walshaw, 1984). Theoretically, the amount of damping which exists between the wobbling mass and the rigid mass of the leg, could be determined using this method. However, determination of the oscillatory motion of the wobbling mass, relative to the rigid mass, does not necessarily require the determination of the visco-elastic properties within the system, despite the fact that it is these properties which, in part, determine how the wobbling mass will ultimately behave. The resultant, external motion of the wobbling mass, relative to the rigid mass, can be determined by alternative means, including accelerometry.

Accelerometry

To directly measure the accelerations of body segments, or joints, without the corresponding errors associated with taking the second derivative of displacement data, accelerometers can be used. The use of accelerometers

for these purposes however, is also not without its limitations. The location and method of accelerometer attachment to the body are issues that must be considered.

Mounting accelerometers directly to the skin overlying soft tissue allows for the accelerometer to move with respect to the underlying tissue (muscle), and can therefore register movement even in an isometric contraction (Willemsen et al., 1990). Movement of the accelerometer is also an issue when it is mounted on skin which overlies bone. In this case however, tissue movement can be greatly reduced depending on the method of attachment.

Numerous methods for accelerometer attachment have been reported in the literature. Fixation of accelerometers to metal pins which are imbedded directly into bone will reduce the effects of soft tissue movement (Light and McLellan, 1977; Light et al., 1980; Lafortune and Hennig, 1991; Hennig and Lafortune, 1991), but involves invasive surgical techniques and is a major time commitment when compared to other methods. Fixation of topical accelerometers, to skin and to bone, has been done using a variety of other methods including needles inserted to the bone surface through the overlying soft tissue (Ziegert and Lewis, 1979) elastic straps (Ziegert and Lewis, 1979; Voloshin and Wosk, 1981; Voloshin and Wosk, 1982; Mizrahi and Susak, 1982a), high friction casts (Morris, 1973), and aluminum

brackets (Gilbert et al., 1984; Willemsen et al., 1990).

Tight fixation of the accelerometer over the soft tissue of a segment will provide a form of mechanical damping, a technique chosen in some cases in order to reduce the effects of soft tissue movement (Morris, 1973; Ziegert and Lewis, 1979; Gilbert et al., 1984). Ziegert and Lewis (1979), investigated the relative movements of the tibia and overlying soft tissues of the anterior leg following distal tibial perturbations, by comparing the acceleration/time histories of two skin mounted accelerometers of different mass (1.5 and 34 gram), to the output of an accelerometer mounted firmly to the anterior tibia (surface accelerometers were secured using elastic straps). It was found that the high mass accelerometer (34 gram), despite being secured tightly around the leg with an elastic strap, registered the relative low frequency motion of the soft tissue over which it was attached. However, the output of the low mass (1.5 gram) accelerometer was nearly the same as the relative high frequency output measured by the tibial mounted accelerometer, following distal tibial vibration. This indicates that the strapping down of the low mass accelerometer provided sufficient damping of the soft tissue motion, between the anterior tibia and the accelerometer, such that the accelerometer could accurately measure the actual tibial accelerations resulting from the high frequency impacts at the

distal end of the segment. This method has been used by numerous investigators interested in accurate, non-invasive measurements of skeletal accelerations following external system perturbations (Light et al., 1980; Voloshin and Wosk, 1981; Voloshin and Wosk, 1982).

The effect that the elastic strapping had on the motion of the posterior leg soft tissue, was not investigated in the study by Ziegert and Lewis (1979), however, the results suggest that elastic strapping would directly interfere with the independent motion of the soft tissue mass. If a surface accelerometer is being used to measure the effect that soft tissue movement has on body motion (Mizrahi and Susak, 1982a), then it seems evident that fixation of the accelerometer should not interfere with the soft tissue motion.

Summary

Following review of the above literature, it seems evident that the independent movement of lower extremity wobbling mass has an effect on reducing the transmission of peak forces to the knee joint as a result of impacts with the ground. The magnitude of the effect however, is still unknown. Also, it has been shown that the relative contributions of rigid and wobbling masses of the leg to the overall oscillatory response of the leg, following impact with the ground, can be quantitatively measured with accuracy using

low mass, skin mounted accelerometers. These findings suggest that the failure to include wobbling mass components in link segment models, whose purposes are to describe the response of the human body following the introduction of large external forces (and hence accelerations), may contribute to inaccurate, or at least, less than realistic results.

METHODS

Subjects

Fifteen healthy subjects (8 male and 7 female) participated in this study (mean age = 23.8 years; mean mass = 73.0 kg). All subjects were required to sign an informed consent form and were screened for any lower extremity joint or tissue injuries prior to participation. The experimental protocol was described to each subject prior to testing.

Testing Apparatus and Task

A testing apparatus to the one used by Mizrahi and Susak (1982b), was made for the purposes of this experiment. The experimental apparatus used for subject data collection is shown in Figures 2a and 2b. A metal bar was supported by two ropes suspended from the metal framework in the ceiling of the laboratory, directly above the force platform. The height of the bar above the force platform was adjusted for each subject such that the soles of their bare feet were raised the required distance, either 5 or 10 cm above the force platform when hanging by fully extended arms from the bar above. Subjects were asked to drop from this position onto the force platform, landing on one leg with the ankle and knee of the support leg locked. The drop heights of 5 and 10 cm were measured by inserting pre-cut blocks of wood of the desired height between the force plate and the subjects feet while

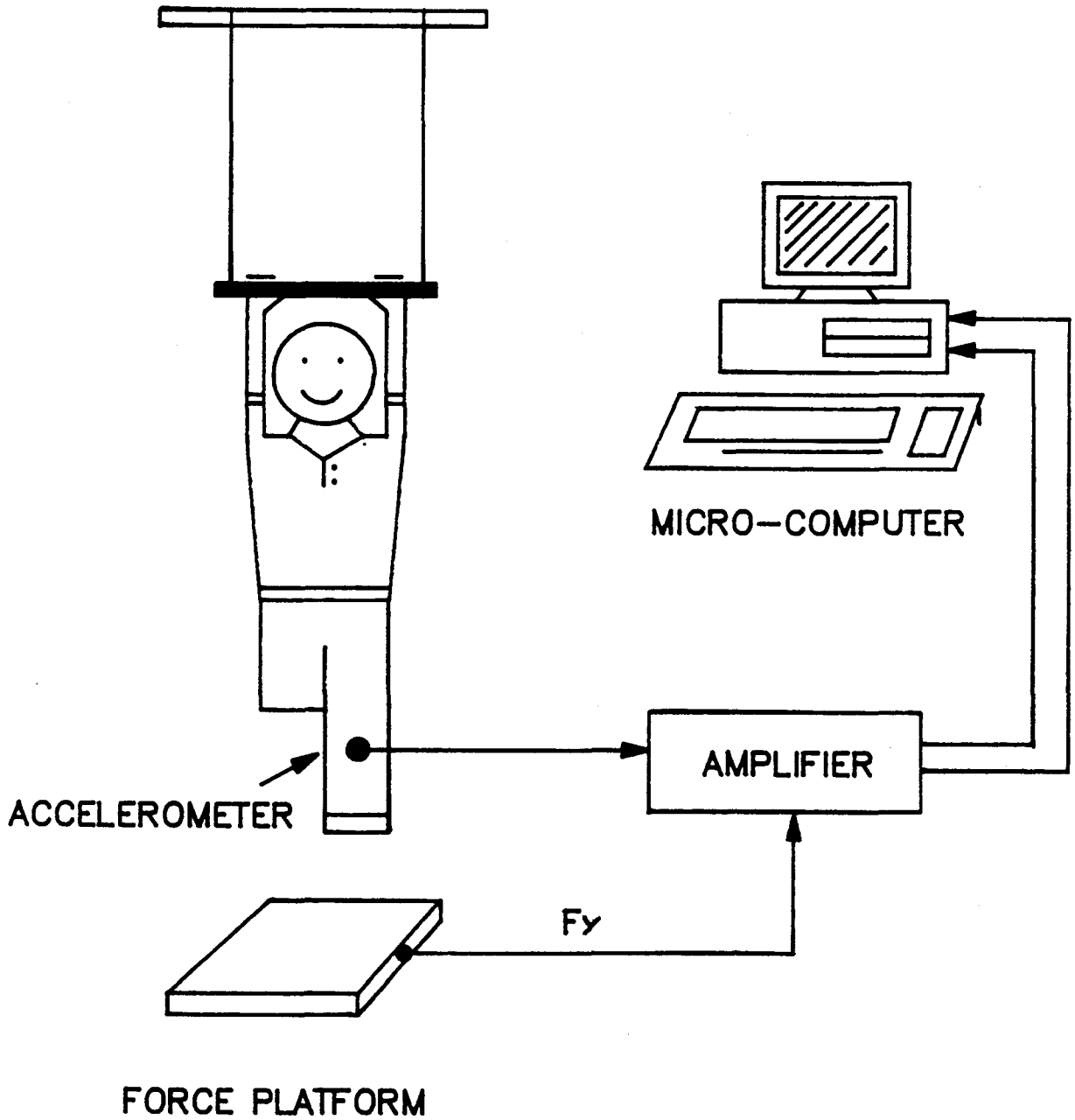


Figure 2a: Diagram of experimental setup for subjects.



Figure 2b: Photograph of one subject hanging on the actual experimental apparatus.

they hanged from the bar.

The Mechanical Model

A schematic diagram of the mechanical model which was designed (by the author), and manufactured (Department of Engineering, McMaster University), to measure actual vertical knee joint reaction forces following impact with the ground, is shown in Figure 3a. Figure 3b is a photograph of the actual mechanical model, and Figure 3c schematically depicts the model's visco-elastic components.

(i) Components

The foot of the support leg was modelled as a flat plate, and was attached rigidly at the ankle joint to the rigid portion of the leg.

The non-rigid or wobbling mass component of the leg was attached to the rigid portion of the leg such that it hanged much like the wobbling mass of an actual human leg, but from a cantilever rod on the posterior aspect of the leg (Figure 4). The oscillatory motion of the wobbling mass was constrained to the vertical direction by the introduction of a pin guiding system between the rigid and non-rigid masses of the leg. The pin guiding system provided some amount of friction damping to the oscillations induced by impact with the ground.

The knee joint of the model consisted of a load cell rigidly attached to the rigid portions of the leg and foot

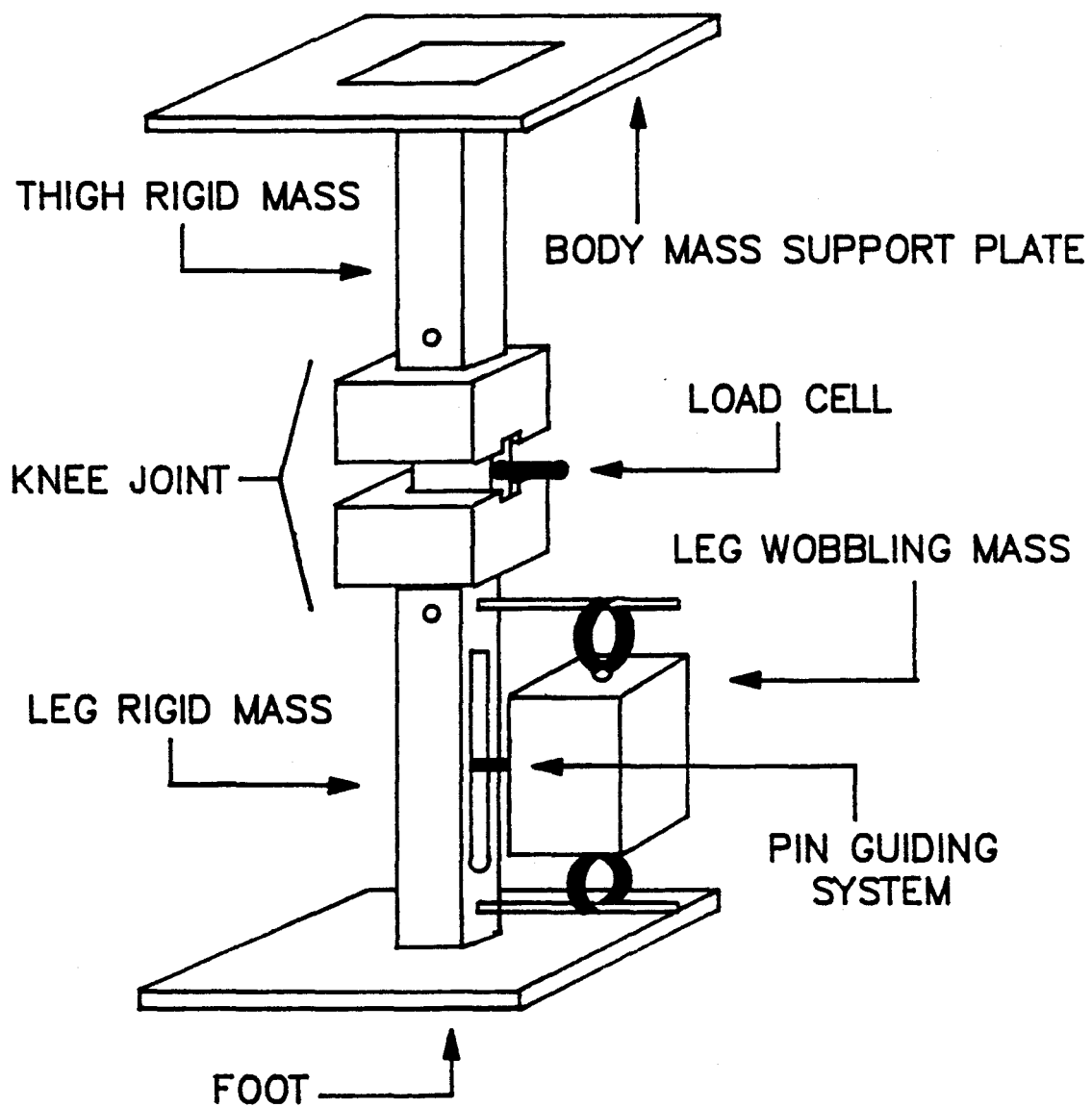


Figure 3a: Schematic diagram of manufactured mechanical model.

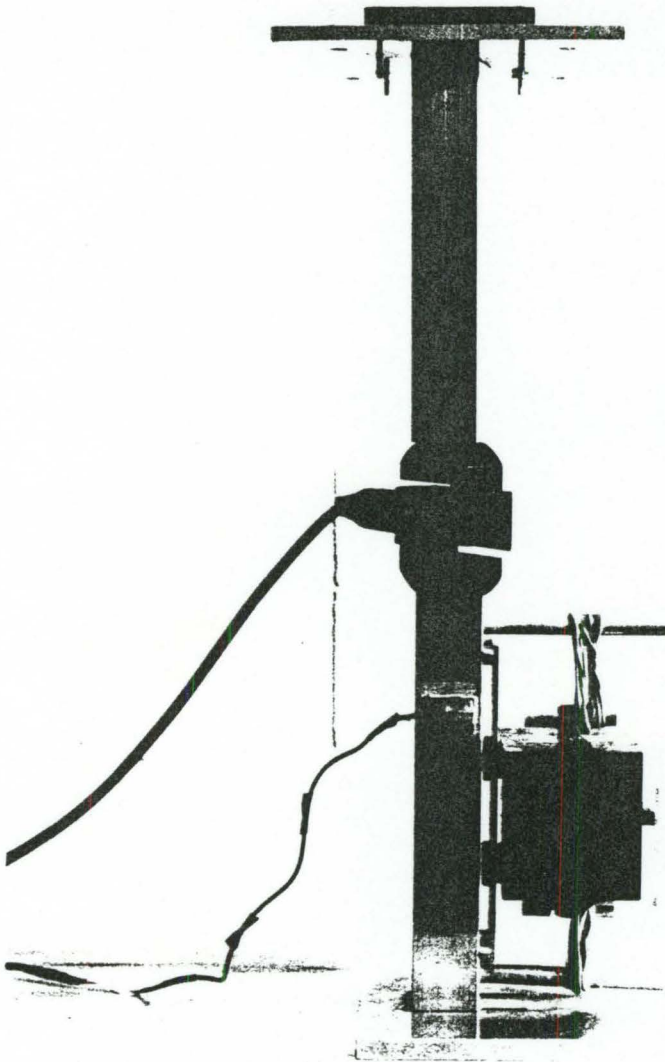


Figure 3b: Photograph of the actual mechanical model.

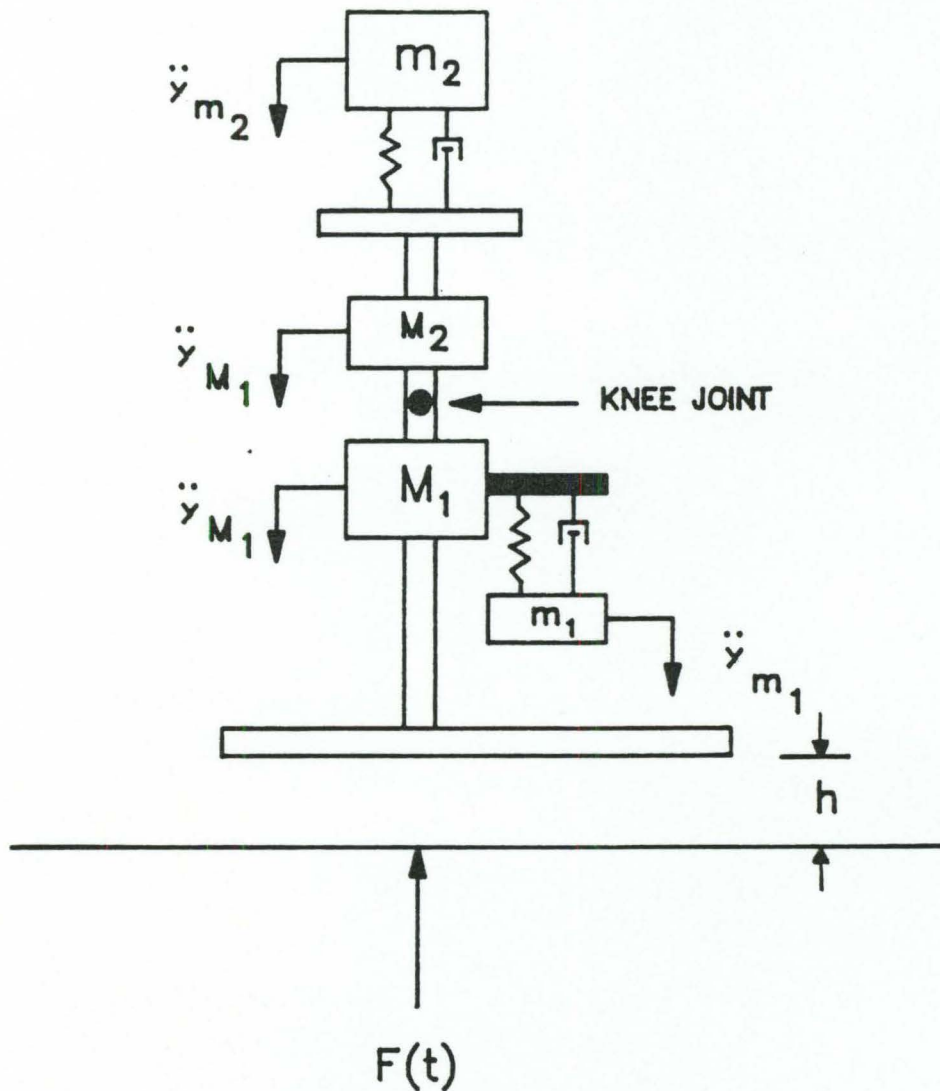


Figure 3c: A schematic diagram of the rigid and wobbling mechanical model. M_1 and M_2 are rigid masses representing the leg and foot section and the thigh section, respectively. m_1 and m_2 are the wobbling mass sections of the foot and leg and the trunk, respectively. The \ddot{y} 's are linear accelerations.

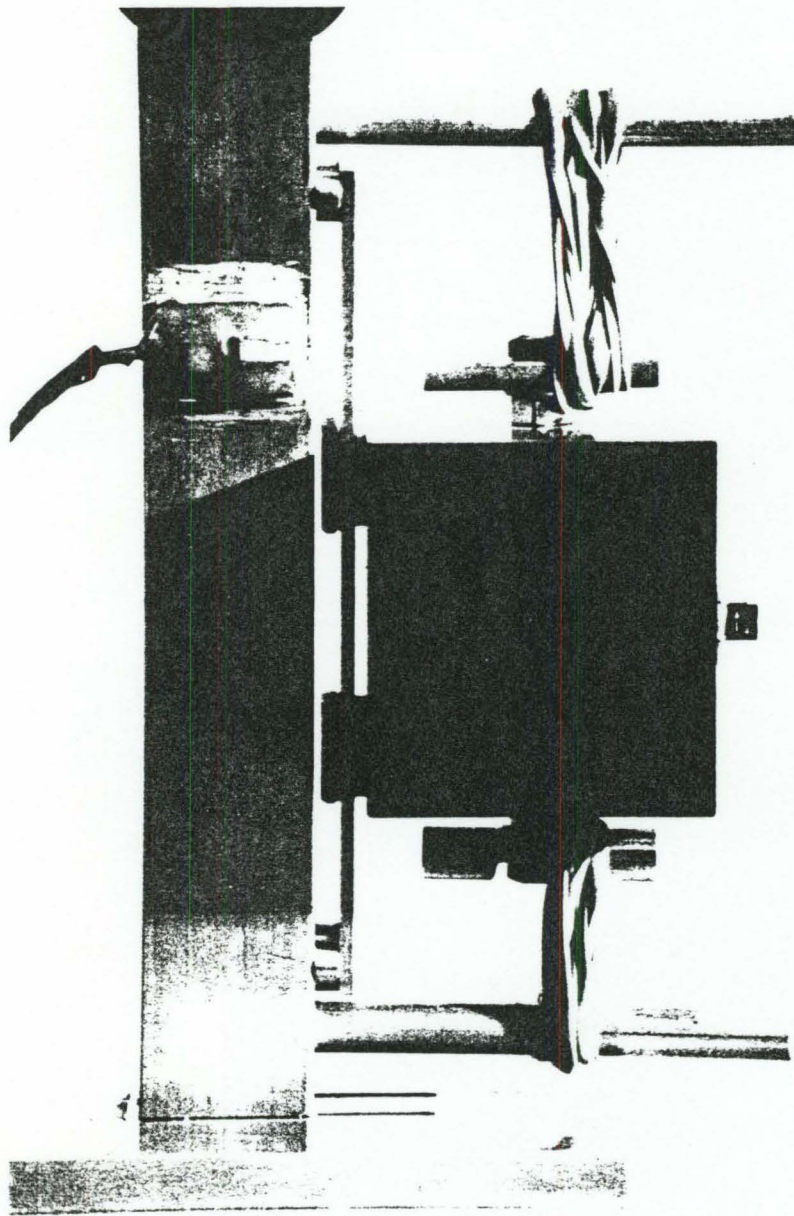


Figure 4: Photograph showing lower portion of the mechanical model including the wobbling mass portion, on the posterior aspect of the rigid leg; the pin guiding system; and the elastic band connections.

segment below the joint, and the thigh segment above the joint. The load cell was the means of determining the vertical joint reaction force at the knee.

The construction of the rigid portion of the thigh segment was similar to that of the leg segment. A plate similar to the foot was placed on the top end of the rigid thigh segment. On this surface, additional mass was positioned, in order to model the thigh and trunk mass, and the concomitant visco-elastic effects associated with that mass.

Vertical, and motionless suspension of the mechanical model prior to release was important to ensure vertical flight. A quick release mechanism, using an electromagnet, was utilized to support the model prior to release such that it did not alter the model's downward flight when dropped (Figures 5a and 5b).

The magnitudes of the independent movements of the rigid and wobbling mass portions of the leg and foot segment were obtained by accelerometry. Two piezoresistive accelerometers were mounted on the leg segment as follows. The first accelerometer was secured to the rigid portion of the leg on the anterior, superior surface of the rigid leg segment. (The vertical acceleration of the rigid section of the leg was assumed to be constant at all points on it because it was rigid. It was also assumed that dropping the

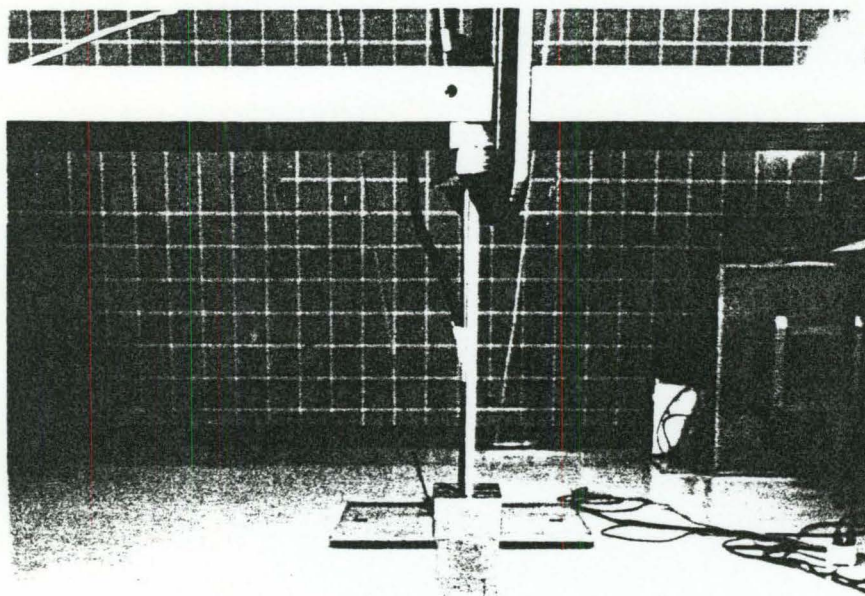


Figure 5a: A photograph showing the quick release apparatus, with electro-magnet, used to suspend and then release the mechanical model.

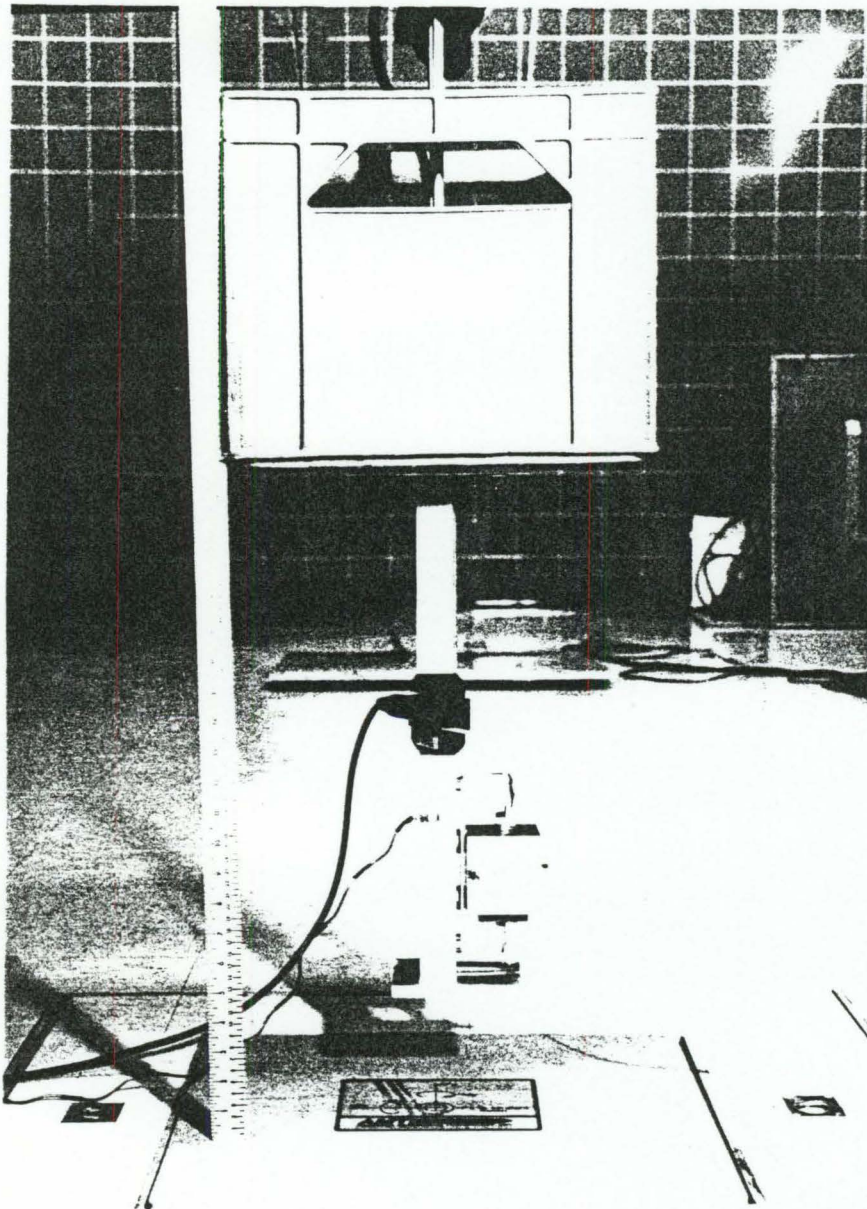


Figure 5b: A photograph depicting the mechanical model suspended by the quick release apparatus.

model vertically downwards eliminated any tibial angular acceleration). The second accelerometer was fixed to the wobbling mass portion of the leg, on the posterior aspect of the leg.

(ii) Segment Parameters

The construction of the mechanical model was done such that segment lengths, total mass, and component tissue mass was in proportion to those from human cadaver data, relative to a human of mass 75 kg. The determination of these relevant anthropometric measures is discussed below.

(iii) Materials

The rigid mass portions of the model (which include the foot, leg, thigh, and the cantilever beams from which the wobbling masses are suspended), were constructed of aluminum metal. The wobbling mass portion of the leg segment of the model was made of steel.

The connection between the rigid and wobbling masses was made via the pin guiding system and numerous tightly wound rubber elastic bands.

The above knee wobbling mass (representing the thigh and trunk) consisted of about 16 kg of bean bags and bagged rice. These materials functioned, to some degree, in damping the vertical bounce of the model, which occurred following impact with the force platform. The bean bags and rice were housed in a plastic milk crate which in turn was bolted to the

aluminum plate on the superior aspect of the rigid portion of the thigh.

Several pilot experiments were performed (which consisted of dropping the mechanical model while systematically varying the stiffnesses of the elastic bands, the amount of friction damping inherent in the pin guiding system, as well as the amount and distribution of the above knee wobbling mass) such that the rigid and wobbling mass accelerations, and ground reaction force waveforms, of the model, most closely reflected those exhibited by human subjects.

The actual and calculated ideal (as per cadaver data for a subject with mass 75 kg) masses of the rigid and wobbling components of the mechanical model are presented, for comparison, in Table 1.

Equations of Motion

Figure 6 shows a free body diagram of a combined rigid and non-rigid leg in dynamic equilibrium. Since the leg was in dynamic equilibrium at impact, the overall equation of motion of the leg was represented by Equation [4].

Rearranging Equation [4] and substituting in for \ddot{y}_3 from Equation [5], and for \underline{m}_3 from Equation [6], the vertical knee joint reaction force R_y , was determined.

Table 1: Actual and calculated ideal masses of rigid and wobbling components of the mechanical model. (Ideal masses calculated for a 75 kg human, as per data from Clarys and Marfell-Jones, 1986 and Dempster and Gaughran, 1967).

SEGMENT	IDEAL MASS (kg)	ACTUAL MASS (kg)	ABSOLUTE ERROR (kg)
THIGH (RIGID)	0.73	0.75	+ .02
TRUNK (TOTAL)	19.80	17.60	- 2.20
LEG (RIGID)	0.77	0.83	+ .06
FOOT (RIGID)	0.33	0.32	- .01
LEG AND FOOT (WOBBLING)	2.70	2.54	- .16
TOTALS	24.33	22.04	- 2.29

$$R_Y + F_Y - m_1'g - m_2'g = m_3' \ddot{Y}_3 \quad [4]$$

Where $\ddot{Y}_3 = (m_1' \ddot{Y}_1 + m_2' \ddot{Y}_2) / (m_1 + m_2) \quad [5]$

and $m_3 = m_1 + m_2 \quad [6]$

Determination of the vertical knee joint reaction force R_Y , using a completely rigid leg segment was done the same as above. However, Equation [4] was reduced to give Equation [7].

$$R_Y + F_Y - m'g = m' \ddot{Y}_3 \quad [7]$$

Where $\ddot{Y}_3 =$ acceleration of the leg center of gravity.

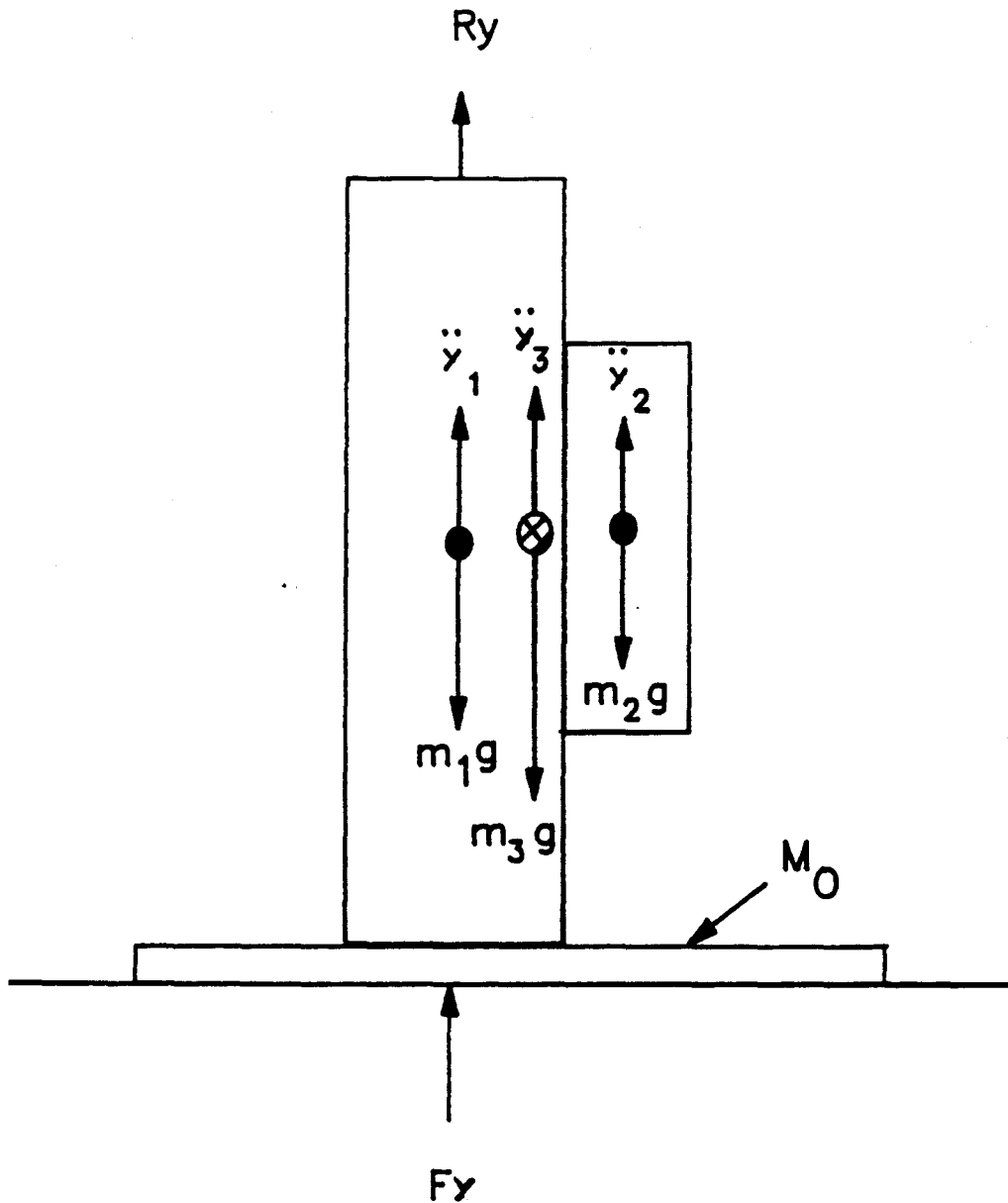


Figure 6: A free body diagram of a rigid and wobbling leg in dynamic equilibrium. Values for F_y are from the force platform, and accelerations \ddot{y}_1 and \ddot{y}_2 are from surface mounted accelerometers. \ddot{y}_3 is the resultant linear acceleration of the combined model. The mass of the rigid section is m_1 , the wobbling section m_2 , and m_3 is the total mass of the system. The mass of the supporting foot (m_4), is part of the rigid mass m_1 . R_y is the vertical knee joint reaction force.

Determination of Subject Anthropometrics

The magnitudes of rigid and wobbling tissue masses per total segment mass for the foot and leg, and thigh was obtained from the cadaver data reported by Clarys and Marfell-Jones, (1986a). The total mass of each segment was determined from cadaver data reported by Dempster and Gaughran (1967). In order to use any of the above mentioned cadaver data, the total body mass of each subject was measured.

Data Collection

Subjects

(i) Force platform

The ground reaction force in the vertical direction (F_y) was collected using an AMTI force platform (model #OR6-5), for 1 second following release of the subject from the support bar. The natural frequency of the force platform was determined to be approximately 260 Hz. Force platform data were channelled to an analog to digital (A/D) data acquisition system (Northern Digital) and was sampled at a rate of 1000 Hz. These data were stored on disk and on a micro-computer (Amdek, 286).

(ii) Accelerometry

The vertical accelerations of the rigid and wobbling tissue of the leg were measured by a 1000g and a 50g piezoresistive accelerometer (Durham Instruments), respectively. The accelerometers were secured, by Skin Bond

Cement (an adhesive by Smith and Nephew; used specifically in Enterostomal Medicine), to the skin overlying the superior, anterior surface of the tibia, and the gastrocnemius muscle respectively, as shown in Figure 7. Acceleration signals from the two channels were amplified (Honeywell and Durham Instruments) and then A/D converted at a sampling rate of 1000 Hz for 1 second following release of the subject from the support bar. Data were stored on a micro-computer. (Since it was the accelerations of the tissues following impact with the force platform that were of interest in this study, acceleration data prior to impact was not analyzed).

(iii) Electromyography (EMG)

Bipolar disposable Ag/AgCl surface EMG electrodes (3M) were attached to prepared skin (shaved, roughened and swabbed with alcohol) over the bellies of, medial gastrocnemius (G), tibialis anterior (TA), biceps femoris (H), and vastus lateralis (VL) of two of the 15 subjects. The interelectrode distance for each set of electrodes was about 2.0 cm, and the electrical impedance following skin preparation was always below 20 k Ω . The electrical activity of each muscle was collected at 1000 Hz. for 2 seconds during three trials from a drop height of 10 cm. The two subjects performed maximal voluntary contractions (MVCs) and relaxed trials for each muscle for calibration purposes. EMG data were pre-amplified (CMRR > 90 dB; bandwidth 10-500 Hz; input impedance 100 M Ω) and

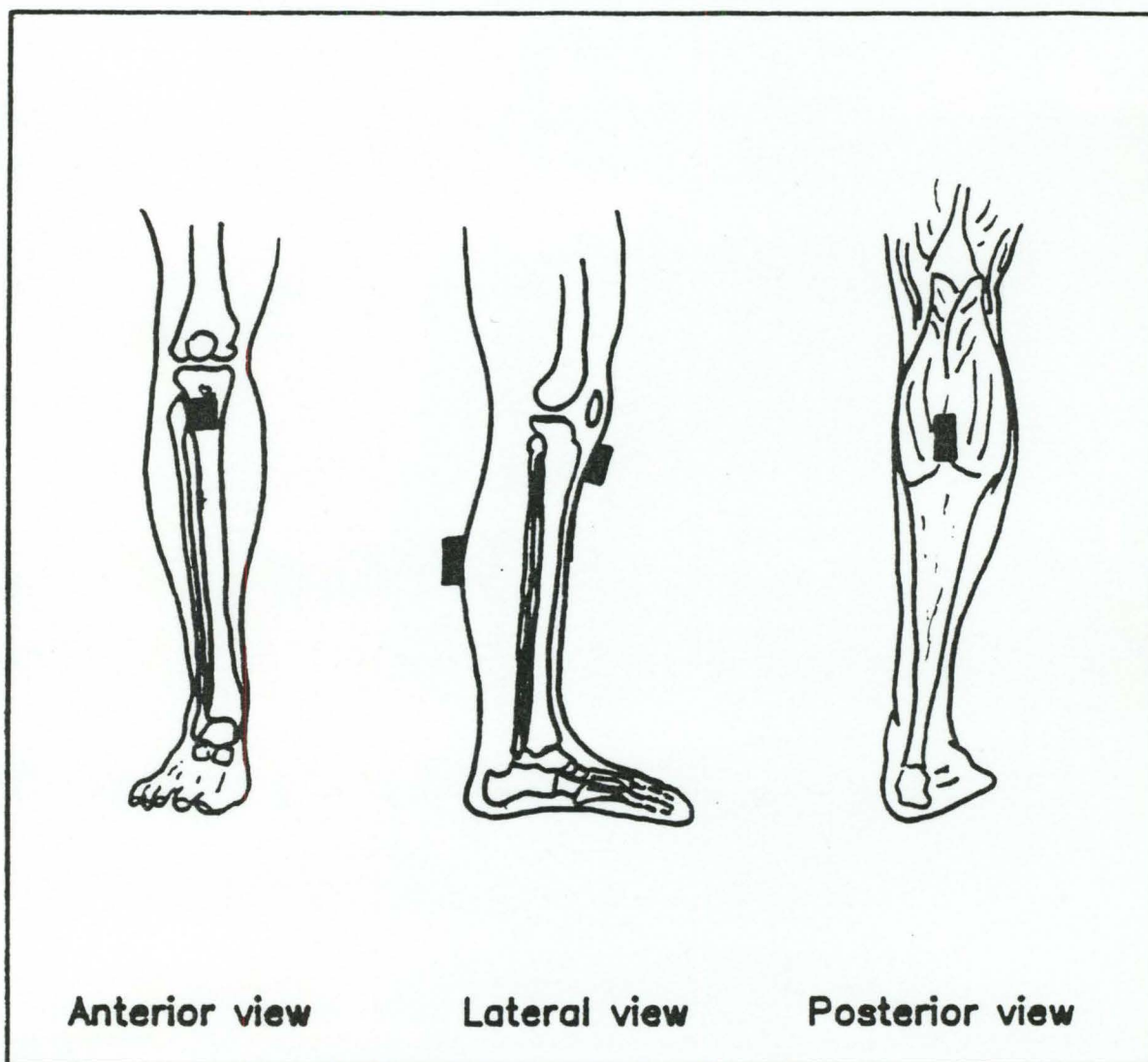


Figure 7: Accelerometer mounting sites on the rigid and wobbling sections of the leg.

then A/D converted and stored in the same manner as were accelerometer and force platform data.

Model

(i) Force Platform

For validation purposes (see below), the manufactured model was dropped from the same heights (5 and 10 cm) as were the subjects. Force platform data for the mechanical model was collected as per subject criteria.

(ii) Accelerometry

Acceleration data for the mechanical model was also collected as per subject criteria.

(iii) Load Cell

Vertical knee joint reaction force data was measured at a rate of 1000 Hz. for 1 second following release of the model from the electromagnet (Jobmaster Magnets) using a load cell (Durham Instruments) mounted between the rigid portions of the leg and thigh. Load cell signals were amplified (Durham Instruments) and then collected as per subject data criteria.

Data from a total of 3 channels, over 6 trials, were collected for each subject. (2 drop heights \times 3 attempts per height = 6 trials). Subjects were encouraged to land with a stiff ankle and knee for each trial. Practice executing the task without loss of balance upon impact with the force

platform, was allowed at any time during the testing protocol as required by the subject.

Data from a total of 4 channels, over 6 trials, were collected for the mechanical model. (2 drop heights x 3 attempts per height = 6 trials).

Data from a total of 5 channels (4 EMG channels and the force platform channel as a time reference), over 3 trials, were additionally collected for two subjects. (1 drop height x 3 attempts at each height = 3 trails).

Model Validation

Proceeding on the assumption that subject VKJRFs which were calculated using the rigid-only and the rigid and wobbling equations of motion (Equations [7] and [4]) would differ from one another following impact, the mechanical model was manufactured to provide actual VKJRFs to which the estimated subject values could be compared. By definition then, the comparisons of actual VKJRFs from the model to the estimated subject VKJRFs provided an indirect validation of the subject results. In addition, the comparison of actual VKJRFs from the model to estimated model VKJRFs (calculated as per subjects) provided a direct validation of the model estimated results.

Data Analysis

(i) Rigid and Wobbling Mass Accelerations

The rigid mass and wobbling mass acceleration

waveforms for all subjects, and for the mechanical model, were analyzed to give values for initial peak acceleration (IPA), and duration from impact to baseline. IPA values were expressed in terms of gravity (g), and waveform durations in units of ms.

(ii) Vertical Ground Reaction Forces (GRF)

The vertical GRFs for each subject, and for the mechanical model, were analyzed to give values for peak force (PF) and time to peak force, or rise time (RT). PF values were expressed in terms of body weight, and RT values in units of ms.

(iii) Vertical Knee Joint Reaction Forces (VKJRF)

The accelerometer and ground reaction force data from all trials for each subject, and for the mechanical model, were used in the calculations of vertical knee joint reaction forces (VKJRF). Calculations were done as per Equations [4]-[7]. The resultant VKJRFs, using both calculation methods, were expressed in terms of body weight.

(iv) Electromyographical Activity

The EMG signals from each of the muscles G, TA, H, and VL, for each of the two subjects, were full wave rectified, and low pass filtered (critically damped, single pass) at a cut-off frequency of 3 Hz. The percent activation of each muscle, with respect to MVC, was determined at impact. The time of peak muscle activity (PAT), was also determined with

respect to the time of impact, which was arbitrarily designated as time equal to zero. Time prior to impact was designated negative, and following impact was positive. The activity level of muscles that showed continual activity throughout the trial were also determined as a percentage of the MVC of that muscle.

Statistical Measures

Subjects (n=15)

Mean IPA, acceleration waveform durations, PF, and RT values (\pm standard deviations) were determined for all subjects at each of the drop heights.

The %RMS errors and correlation coefficients (\underline{r} values) of estimated VKJRFs of each subject, using the rigid-only, and combined rigid and non-rigid link segment methods, were determined. Mean %RMS errors (\pm standard deviations) and \underline{r} values were then calculated for each subject at each of the drop heights, for both the rigid-only and rigid and wobbling models.

Mean peak VKJRFs (\pm standard deviations) were calculated for each subject, at each of the two drop heights, using both calculation methods. A two factor (factor 1 = height and factor 2 = method) repeated measures ANOVA was used to test for significance between the mean peak values, with $\alpha < 0.05$.

EMG Subjects (n=2)

Mean values (\pm standard deviations) for percent activation at impact, PAT and continual activity percentage were determined for each of the two subjects across three trials at the drop height of 10 cm.

Model

The "goodness of fit" between each of the actual VKJRF curves (from the load cell), and the two estimated VKJRF curves (obtained by using rigid-only and combined rigid and wobbling link segment calculations), was determined by using %RMS errors and correlation coefficients (r values). Mean %RMS errors and r values (\pm standard deviations) were then calculated at each of the drop heights.

Mean actual and estimated peak VKJRFs (\pm standard deviations) were also calculated for the model at each drop height. The absolute differences between these means were noted.

RESULTS

Subjects

(i) Rigid and Wobbling Mass Accelerations

The rigid and wobbling mass accelerations of a trial for a typical subject are shown in Figures 8a and 8b, respectively. Time of impact is denoted by the vertical line crossing each part of Figure 8. The rigid and wobbling acceleration waveforms for all subjects had the characteristic shape of those seen in Figure 8, with an initial large peak acceleration followed by a smaller second peak, opposite in sign. All waveforms then returned to baseline with varying numbers of oscillations and at varying rates. Mean values for initial peak accelerations (IPAs) and waveform durations from impact to baseline, for all subjects, and at both of the drop heights are included in Table 2.

Table 2: Mean absolute rigid and wobbling mass acceleration results for all subjects (n=15).

ACCELEROMETER	HEIGHT (cm)	MEAN INITIAL PEAK ACCELERATION (g) \pm SD	MEAN DURATION: IMPACT TO BASELINE (ms) \pm SD
RIGID MASS	5	22.7 \pm 8.9	129.4 \pm 40.2
	10	31.8 \pm 13.3	126.3 \pm 42.3
WOBBLING MASS	5	23.7 \pm 8.4	159.4 \pm 38.9
	10	32.2 \pm 12.4	158.6 \pm 46.0

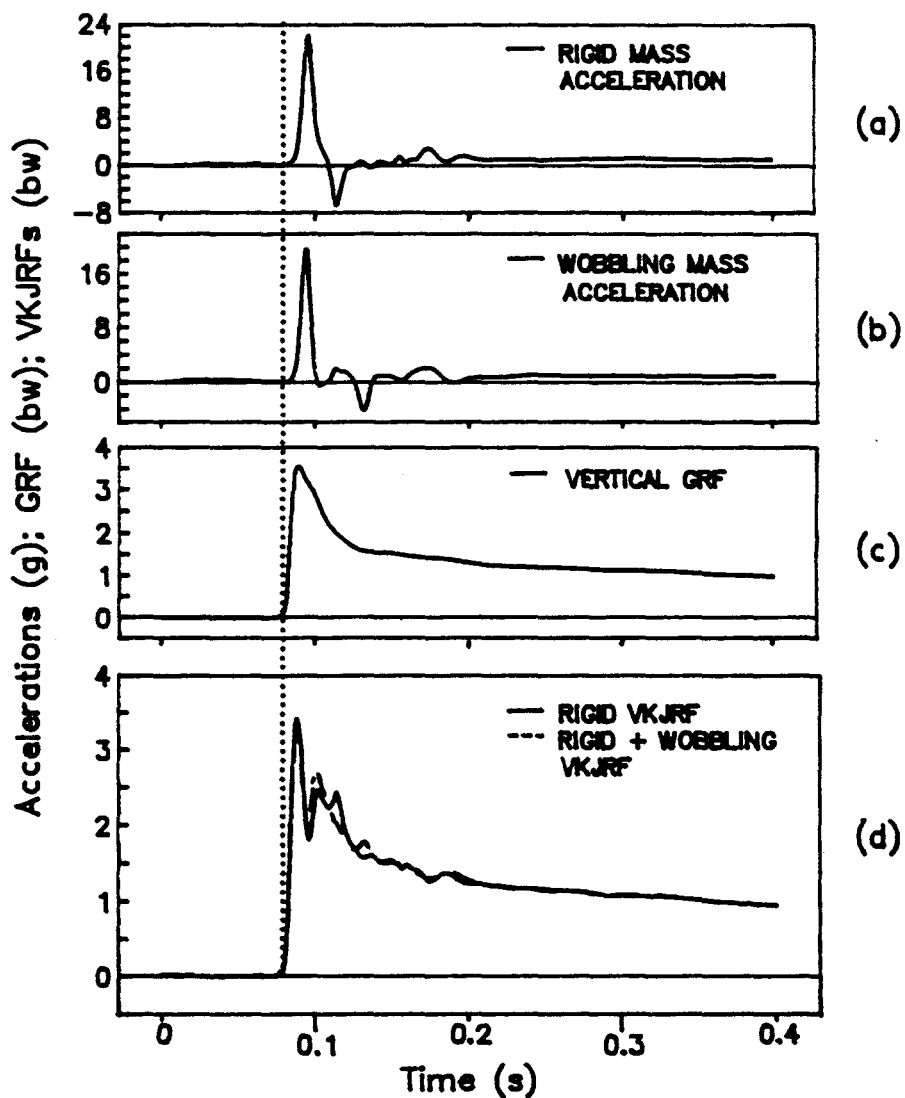


Figure 8: Rigid mass and wobbling mass acceleration curves (a) and (b), ground reaction force curve (c), and corresponding VKJRFs (d), for one trial of a typical subject. Impact with the force platform is denoted by the vertical line drawn through each portion of the figure.

As indicated in Table 2, the magnitudes of the IPAs for the wobbling mass and rigid mass are very similar when dropped from the same height. Mean IPAs were greater (by about 48% for the rigid mass and 36% for the wobbling mass) when dropped from 10 cm as compared to at 5 cm.

On average, the wobbling mass accelerations required about 30 ms more time to return to baseline following impact than did the rigid mass accelerations. This was typically a result of the greater number of waveform oscillations which were noted to follow the second peak in the wobbling mass accelerations, as compared to the rigid mass accelerations (this is not seen in Figures 8a or 8b).

(ii) Vertical Ground Reaction Forces (GRF)

The GRF curve which corresponds to the accelerations shown in Figures 8a and 8b, is shown in Figure 8c. GRF curves were found to be highly repeatable for each subject at each of the drop heights, with an initial high frequency peak of force followed by a rapid and damped oscillation back to body weight. Mean absolute peak forces (PF) and mean rise times (RT), for all subjects at each of the drop heights, are included in Table 3.

As expected, the mean PF was found to be greater in the 10 cm condition ($3.73 \pm .63 \times bw$) than in the 5 cm condition ($2.87 \pm .49 \times bw$). The mean RT to PF was shorter when dropped from 10 cm than it was from 5 cm, but only by about 2.14 ms,

Table 3: Mean absolute ground reaction force results for all subjects (n=15).

DROP HEIGHT (cm)	MEAN PEAK FORCE MAGNITUDE (bw) \pm SD	MEAN TIME TO PEAK FORCE (ms) \pm SD
5	2.87 \pm .49	9.91 \pm 4.81
10	3.73 \pm .63	7.77 \pm 2.65

on average.

(iii) Vertical Knee Joint Reaction Forces (VKJRF)

Figure 8d shows the resultant VKJRF curves which correspond to the accelerations and GRF shown in Figures 8a through 8c. The solid and hatched curves were generated using the rigid-only and the rigid and wobbling equations of motion (Equations [4]-[7], respectively). Enlargements of the VKJRF curves in Figure 8d, are shown in Figure 9.

The VKJRF curves were similar in form for all subjects, with characteristic smaller magnitude second peaks following the initial peak force value, and preceding a fairly rapid return of VKJRFs to baseline values. The return to baseline was typically less than 250 ms after the initial peak.

As indicated by the nearly complete overlapping of the curves in Figure 9, the rigid-only and the rigid and wobbling VKJRF curves were found to be highly correlated with mean r values of 0.979 \pm .015 at the 5 cm height, and 0.976 \pm .013 at the 10 cm height (Table 4). Mean %RMS errors were 19.9 \pm 6.81% x bw

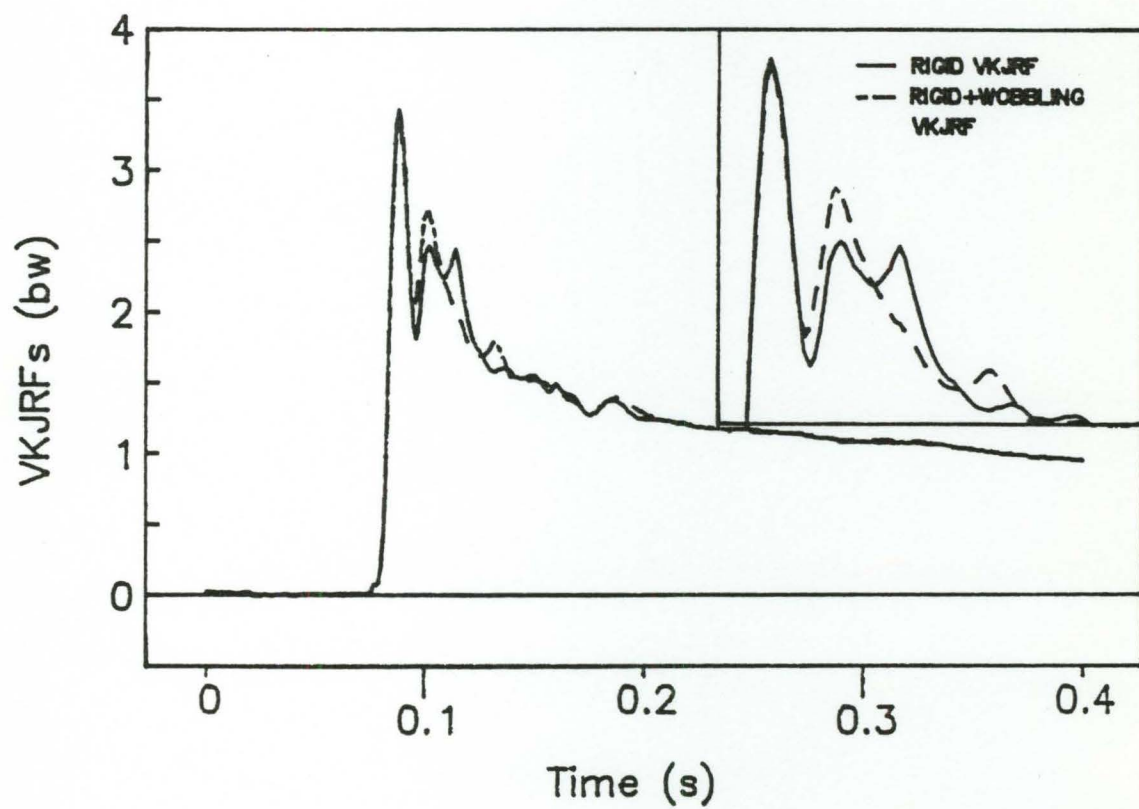


Figure 9: Enlargements of the VKJRF curves shown in Figure 8d.

and $21.1 \pm 5.96\%$ x bw at 5 cm and 10 cm, respectively. Most of the difference between the rigid and rigid and wobbling VKJRF curves were found to occur at, and immediately after the time of the second peaks (see inset of Figure 9). The VKJRF curves typically matched very well temporally and in magnitude at the times of the initial peaks, at both of the drop heights (Table 4).

Table 4: Mean absolute subject VKJRF data. (RRy = rigid only; RWRy = rigid and wobbling).

HEIGHT (cm)	%RMS ERROR \pm SD	r VALUE \pm SD	MAX RRY (bw) \pm SD	MAX RWRy (bw) \pm SD
5	19.9 ± 6.81	0.979 ± 0.015	2.66 ± 0.55	2.64 ± 0.55
10	21.1 ± 5.96	0.976 ± 0.013	3.53 ± 0.68	3.52 ± 0.68

A two factor repeated measures ANOVA revealed that there was no main effect for type of model used, but that there was a main effect for height ($p=0.00001$). There was also no interaction between model type and height dropped.

(iv) Electromyographical Activity

The smoothed rectified EMG and GRF data of one subject, for one trial, is shown in Figure 10. Impact with the force platform occurred when the GRF data changed from the baseline of zero x bw. The temporal occurrence of the point of impact is denoted by the vertical line passing through each part of Figure 10.

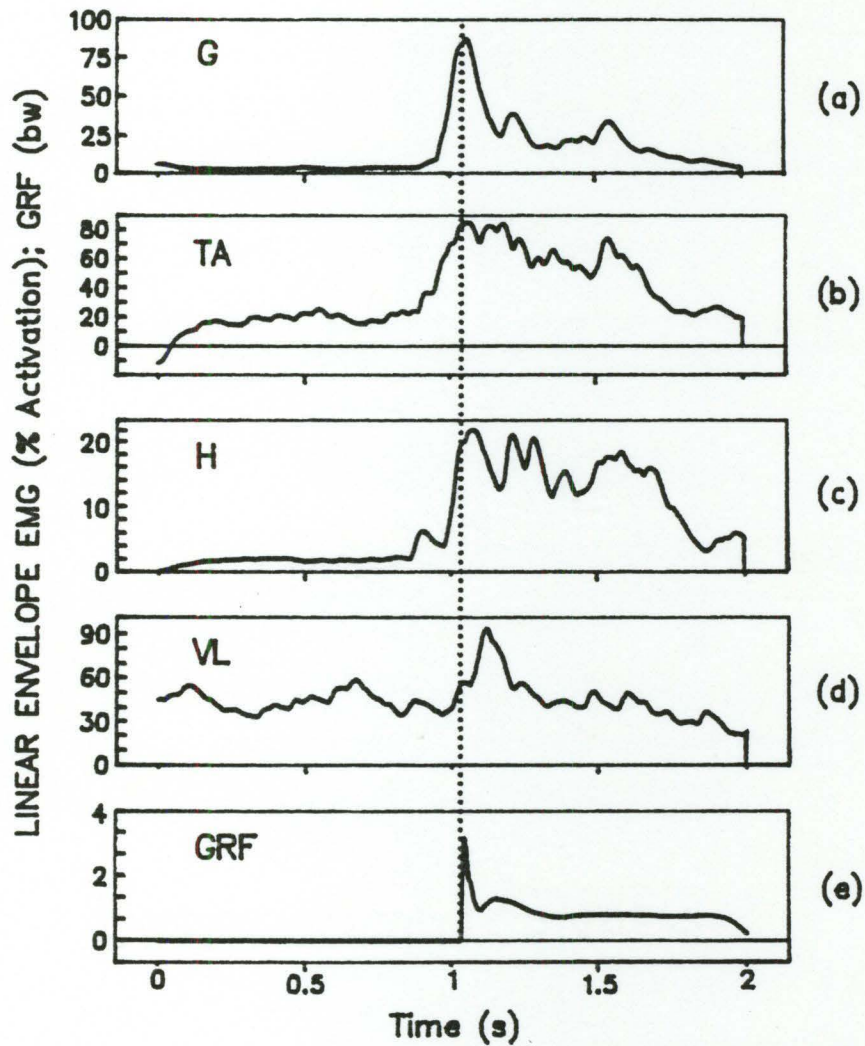


Figure 10: Linear envelope EMG from medial gastrocnemius (a), tibialis anterior (b), biceps femoris (c), and vastus lateralis (d), and the corresponding ground reaction force (e), for one subject. Impact with the force platform is denoted by the vertical line drawn through each portion of the figure.

The mean EMG results of each of the two subjects are shown in Table 5. The mean percent activations at impact for each muscle, and for each of the subjects, indicates that the muscles tested were all active around the time of impact with the force platform. Specifically, tibialis anterior and vastus lateralis were found to be active (mean for TA was 35.9% and 44% for VL) throughout the trials for each of the two subjects. It is also important to note that for all but one of the muscles that had a peak in muscle activity, the peak muscle activity occurred after the time of impact by an

Table 5: Mean EMG results for two subjects landing from 10 cm. Muscles not 'on' throughout (NO), were only minimally active at non-peak times.

SUBJECT	MUSCLE	MEAN % ACTIVATION AT IMPACT ± SD	MEAN TIME OF PEAK ACTIVITY (ms ± IMPACT, + = AFTER) ± SD	MUSCLE ON THROUGHOUT (YES/NO AND %MAGNITUDE)
DA	G	73.0±17.9	+ 13±11.7	NO
	TA	77.9±4.3	+ 121±120	YES, 31.9
	H	23.5±8.7	+ 23±20	NO
	VL	62.2±6.5	+ 76±7.6	YES, 39.7
JD	G	16.5±.9	+ 27±4.9	NO
	TA	42.1±4.7	NO PEAK	YES, 39.8
	H	41.9±5.8	0±15	NO
	VL	63.2±4.8	+ 90±.71	YES, 48.3

average of about 50 ms. Only one of the muscles (H), in one trial for subject JD, showed its peak activity prior to the

time of impact (- 15 ms). In all cases, the medial gastrocnemius (G), and biceps femoris (H) muscles were only minimally active during times not associated with the time of impact (Figure 10).

Model

Unlike the similarities in form and magnitude exhibited in the rigid and wobbling acceleration waveforms, between and within subjects, the accelerations and the ground reaction forces of the manufactured model showed several differences, despite numerous alterations made to the stiffnesses and the damping of the visco-elastic components of the model. The number of manually controlled components that had to be adjusted on the model, made it difficult to obtain consistent and biologically reasonable data, in some cases. This limitation however, did not restrict the usefulness of the model in its ability to provide a comparison between estimated VKJRFs, calculated using rigid-only and rigid and wobbling mass accelerations, and actual VKJRFs, that were measured by the load cell which was fixed at the knee joint of the model.

(i) Rigid and Wobbling Mass Accelerations

Examples of rigid and wobbling mass accelerations of the model, for one trial, are shown in Figure 11a and 11b. Peculiar to the model rigid mass accelerations were second peaks with magnitudes as large, or larger in some cases, as

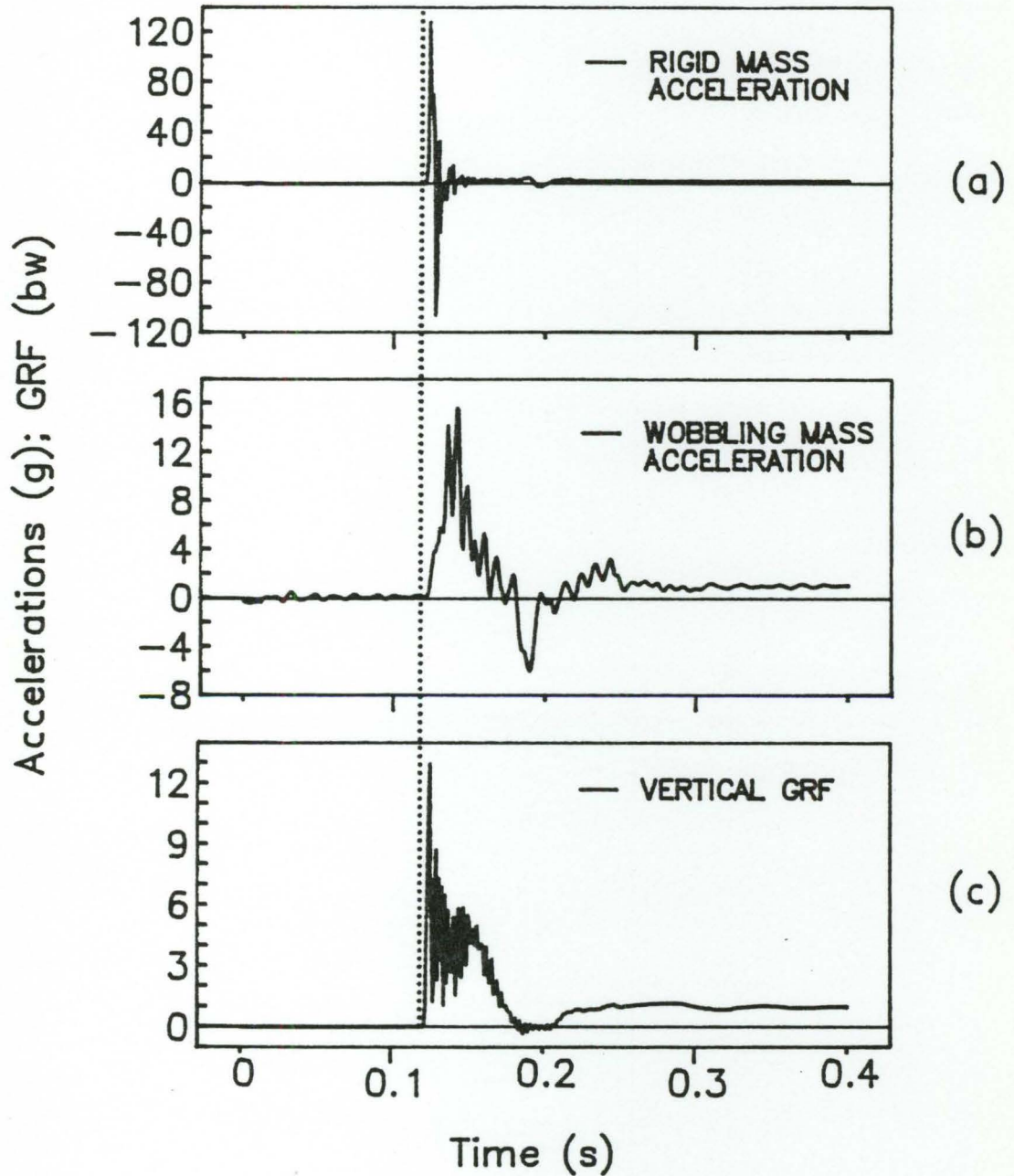


Figure 11: Rigid mass and wobbling mass acceleration curves (a) and (b), and corresponding ground reaction force curve (c), for a typical trial for the model. Impact with the force platform is denoted by the vertical line drawn through each portion of the figure.

the initial peak acceleration values following impact. As indicated in Table 6, the magnitudes of the IPAs were very high, with a mean value of about 4.3 times, and 3.5 times that of the average subject values at 5 cm and 10 cm, respectively.

The mean duration of the rigid mass acceleration waveforms was found to be shorter than for the subjects, by about 90 ms at each of the drop heights. In comparison, the mean durations of the wobbling mass accelerations of the model were about 115 ms and 167 ms longer than were the rigid acceleration values, at 5 cm and at 10 cm, respectively.

Table 6: Mean absolute rigid and wobbling mass acceleration results for the mechanical model.

ACCELEROMETER	HEIGHT (cm)	MEAN INITIAL PEAK ACCELERATION (g) \pm SD	MEAN DURATION: IMPACT TO BASE-LINE (ms) \pm SD
RIGID MASS	5	96.0 \pm 1.7	39.0 \pm 5.6
	10	110.0 \pm 22.6	34.0 \pm 4.0
WOBBLING MASS	5	16.3 \pm 2.1	154.3 \pm 25.9
	10	15.7 \pm 2.5	201.7 \pm 44.0

The wobbling mass accelerations of the model tended to show the same recurring double peaks that were exhibited by the model rigid mass accelerations, and by the subjects, with the following exceptions. The magnitudes of the IPAs were, on average, 7.4 g less than subject values at 5 cm, and 16.5 g less when dropped from 10 cm. The mean durations of the

wobbling mass acceleration waveforms were similar for the model and the subjects at 5 cm, but were greater, for the model, by about 43 ms at 10 cm. In addition, the wobbling mass accelerations of the model were very "noisy", with high frequency vibrations (approximately 75 Hz) on top of an underlying acceleration which more closely resembled those of the subjects.

The rigid mass and wobbling mass accelerations of the model returned rapidly to baseline, following the impact, via damped oscillations. This is especially evident in the rigid mass acceleration curves, like the one shown in Figure 11a.

(ii) Vertical Ground Reaction Forces (GRF)

The GRF curve which corresponds to the accelerations in Figure 11a and 11b, is shown in Figure 11c. The shape of the underlying GRF curves of the model typically showed similar trends when compared with subject curves, with the notable exceptions listed below. Times to peak force (RT) were on average 6.1 ms and 4.0 ms shorter than found for the subjects, at 5 cm and 10 cm, respectively. The mean magnitudes of the peak GRFs were $14.3 \pm 2.52 \times bw$ and $16.7 \pm 3.06 \times bw$ at 5 cm and 10 cm, respectively (Table 7). These values were about 5 times and 4.5 times larger than the subject values at the same heights.

Table 7: Mean absolute ground reaction force results for the mechanical model.

DROP HEIGHT (cm)	MEAN PEAK FORCE MAGNITUDE (bw) \pm SD	MEAN TIME TO PEAK FORCE (ms) \pm SD
5	14.3 \pm 2.52	3.77 \pm .06
10	16.7 \pm 3.06	3.73 \pm .06

Inherent on all the GRF waveforms for the model, was a very high frequency vibration (approximately 200 Hz). The majority of this vibration was seen on the GRF curves just following PF (see Figure 11c).

Following the initial peaks, GRF values typically dropped until the level of zero x bw (unweighting) before rebounding to the level of the baseline (1 x bw). The routine existence of GRFs approaching (or even reaching, in some cases) unweighting, indicates the occurrence of a flight phase, or the tendency of the model to bounce off the force platform following impact. In comparison, the return of subject GRFs to baseline values, showed what seemed to be much greater damping than did the GRFs of the model, at each height.

(iii) Vertical Knee Joint Reaction Forces (VKJRF)

Despite differences in the model accelerations and the GRF waveforms, as compared to those of the subjects, the resultant VKJRFs, calculated using both rigid and wobbling mass accelerations, showed similar shapes to those measured by

the load cell, and from the subjects (Figures 12a-12d). The estimated VKJRFs shown in Figures 12a and 12b correspond to the accelerations and GRF curves in Figures 11a-11c. The mean magnitudes of the initial peak VKJRFs were much closer between the actual load cell values (LCRy) and the estimated rigid and wobbling values (RWRy) than they were between rigid and wobbling (RWRy) and rigid only (RRy), or rigid only (RRy) and actual (LCRy) values (Table 8). In both cases, the estimated VKJRFs overestimated the actual VKJRFs,

Table 8: Mean absolute model VKJRF results (RRy = rigid only; RWRy = rigid and wobbling; LCRy = actual VKJRF measured by the load cell).

HEIGHT (cm)	MAX RRY (bw) ± SD	MAX RWRy (bw) ± SD	MAX LCRy (bw) ± SD
5	22.2±1.0	9.63±.3	7.3±.04
10	23.6±5.6	10.2±1.8	9.0±.4

but to a far less extent than when the wobbling mass accelerations were included in the calculations.

The characteristic shape of the VKJRF curves exhibited by the subjects was not seen in the RRY values, which were generated using only the rigid mass accelerations. The initial VKJRF peaks resulting from rigid segment only calculations, were in the opposite direction when compared to those generated from the combined rigid and wobbling mass accelerations. This dissimilarity in the curves is indicated

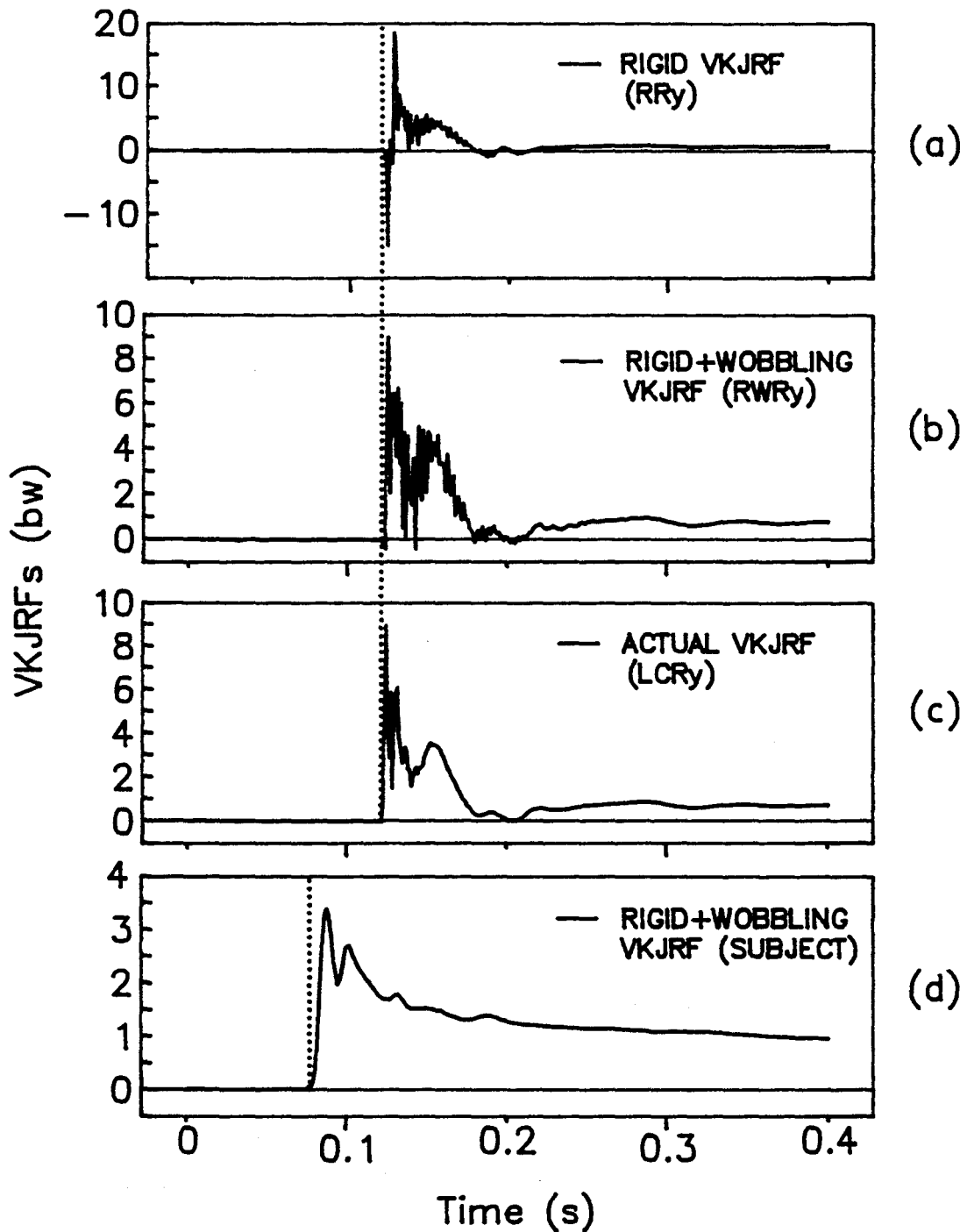


Figure 12: VKJRFs generated using only rigid acceleration (a); VKJRFs generated using rigid and wobbling accelerations (b); actual VKJRFs (c), for a typical trial for the model. Part (d) is a subject VKJRF curve calculated using rigid and wobbling accelerations, for comparison.

by the "goodness of fit" values expressed in Table 9, for actual (LCRy) and estimated (RRy and RWRy) VKJRFs. On average, when the wobbling mass accelerations were included, the

Table 9: Mean "goodness of fit" results for actual (LCRy) and estimated (RRy and RWRy) VKJRFs.

HEIGHT (cm)	VKJRF CURVES FOR COMPARISON	%RMS ERROR \pm SD	r VALUE \pm SD
5	RRy vs. RWRy	78.7 \pm 2.38	0.625 \pm .02
	RRy vs. LCRy	84.4 \pm 9.35	0.538 \pm .16
	RWRy vs. LCRy	70.5 \pm 15.61	0.701 \pm .17
10	RRy vs. RWRy	69.9 \pm 4.91	0.717 \pm .05
	RRy vs. LCRy	79.6 \pm 8.96	0.609 \pm .13
	RWRy vs. LCRy	67.8 \pm 13.56	0.727 \pm .12

estimated VKJRFs were more highly correlated with the actual VKJRFs ($r=0.701\pm.17$ and $r=0.727\pm.12$ at 5 cm and 10 cm, respectively), than when only the rigid accelerations were considered ($r=0.538\pm.16$ and $r=0.609\pm.13$ at 5 cm and 10 cm, respectively). The mean %RMS errors also indicated a poorer fit between the actual and estimated curves when the independent wobbling mass accelerations were omitted.

As a result of the high frequency vibrations shown in the wobbling mass accelerations and the GRFs of the model, estimated VKJRF waveforms also exhibited ringing following the initial peaks. The underlying VKJRF waveforms, RWRy and LCRy, showed the characteristic dual peaks exhibited by subjects,

despite the high frequency vibration on the signals (Figures 12b-12d). Following the second peaks, the return of the estimated and actual VKJRFs to baseline values typically occurred with a drop of values below baseline prior to levelling off. This was not seen in any of the subject data.

Although the mean estimated and actual VKJRFs of the model were much larger in magnitude than those seen in the biological system, these results provide some evidence to suggest the greater accuracy of VKJRFs calculated using both rigid and wobbling accelerations, as compared to rigid mass accelerations alone, at least for the physical model.

DISCUSSION

Subjects

(i) Rigid and Wobbling Mass Accelerations

The similar shapes and peak magnitudes of the rigid mass and the wobbling mass accelerations for the subjects, brings to question the underlying assumption made in this study, that the rigid and wobbling mass portions of the leg accelerate independently, and to different degrees, when large external peak forces are applied. The absence of major differences in rigid mass and wobbling mass accelerations may be explained in several ways. Firstly, for the activity chosen, the wobbling mass components of the leg may have behaved more like rigid mass than first thought. Rigidity of the wobbling mass tissue may have been caused by the conscious, or reflexive generation of tonic activity within the muscle portion of the wobbling mass tissue, in response to joint instability after impact. Secondly, it may have been that the fixation of the accelerometers directly to the skin of subjects lead unknowingly to the measurement of skin movement directly beneath the accelerometer, rather than the accelerations of the underlying rigid and wobbling tissues.

In the activity chosen, subjects were asked to land rigidly on the heel of their support leg such that the natural

shock absorbing properties of the foot arch were not utilized. It was visually evident that to accomplish this task successfully, subjects had to dorsiflex their foot at the ankle while hanging from the bar prior to impact. The electrical activity of tibialis anterior (TA) reflected this observation, being continually active at approximately 36% of maximum, on average, throughout the trial. In addition, by dorsiflexing, subjects were also passively stretching the musculo-tendinous component of the posterior wobbling mass, causing increased rigidity. The role of gastrocnemius (G) in the production of wobbling mass rigidity was inconclusive (due to variable results), despite its tonic state at, and following the time of impact. The neural activation of TA and G, as shown in this study, was interpreted as being an attempt by the leg musculature to maintain joint (knee and ankle) stability. In other similar impact situations, such as in certain ballet movements (Galea and Norman, 1985), cocontractions of leg musculature have commonly occurred for this reason.

For the purposes of this study, fixation of the accelerometers had to be done with minimal interference to the independent motion of the wobbling mass portion of the leg. In addition, to keep the experiments simple, safe, and not aversive to subjects, only non-invasive methods of

accelerometer fixation were considered.

According to Ziegert and Lewis (1979), a low mass accelerometer (1.5 gram) mounted with elastic strapping on the skin overlying the tibia, very accurately reproduced the actual acceleration of the underlying bone. When the mass of the accelerometer was increased to 34 grams, the output of the skin mounted accelerometer more closely resembled the lower frequency acceleration of the underlying soft tissue between the bone and the skin. Although elastic strapping was not used in this study, so that interference with the motion of the wobbling mass could be minimized, a secure and strong union of accelerometer and skin was achieved by using skin bond cement. Ziegert and Lewis (1979) showed that the resonant frequency of the accelerometer mounted on the soft tissue was highly dependent on the mass of the accelerometer, and as a result, they concluded that for most accurate reproductions of the true bone accelerations, from topically fixed accelerometers, low mass accelerometers must be used. The masses of the accelerometers used (4.65 gram and 18.20 gram) in this study, were such that the 4.65 gram accelerometer was always mounted over the rigid mass (tibia) of subjects, and the more massive accelerometer (18.20 gram) was always mounted on the wobbling mass of the support leg.

It would be incorrect to assume that the skin beneath the accelerometers did not move independently of the

underlying rigid and wobbling tissues. An attempt was made however, to minimize skin movement, by selecting an activity which required minimal overall range of motion, and minimal angular motion of the segments about the ankle and knee joints.

Despite their similarities, differences did exist between the rigid and wobbling mass acceleration waveforms of all subjects. For example, the durations of the wobbling mass accelerations were typically longer than those of the rigid mass. This was due, in part, to the consistent presence in the wobbling mass accelerations, of a greater number of oscillations which occurred following the second peaks. This may provide some evidence to suggest that despite the tonic activity of the muscular component of the wobbling mass, the wobbling mass accelerometer was measuring the motion of underlying wobbling tissue independent of the bone. It is also suggested that the relative durations of the wobbling mass acceleration waveforms, as compared to the rigid accelerations, were dependent upon the inherent visco-elastic properties of the wobbling tissue, and its connections with the rigid portion of the leg.

(ii) Vertical Ground Reaction Forces (GRF)

The magnitudes of the peak GRFs in this study were in the order of magnitude of $2.87 \times bw$ to $3.73 \times bw$, at 5 cm and

10 cm, respectively. For the purposes of this discussion, these GRFs were defined as those forces which were transmitted via the rigid and non-rigid tissues of the supporting leg segment, to the knee joint, exclusive of the soft tissue that crosses the joint at the articulating surfaces.

Consider that the force attenuating ability of the rigid and wobbling tissues of the leg were similar to those of the trunk. If this were the case, then it follows from the work of McGill et al. (1989), that the applied forces in this study (whose RTs were considerably lower than the 20 ms RTs quoted by McGill et al.) would be attenuated, to some degree, due to the presence of segmental soft tissues. The magnitudes of the peak transmitted forces were found to be reduced in the present study, by as much as 8% of the magnitudes of the peak applied forces. This however, proved to be the case when the leg segment was considered completely rigid as well as when it was considered partially rigid and partially wobbling.

This finding was not surprising when the limitations of the equations of motion used to generate the VKJRFs (Equations [4] and [7]), were considered. It became evident that even though the independent accelerations of the rigid and wobbling masses were not equivalent for each trial, the resultant joint reaction forces were dominated by the magnitude of the GRFs. (The similar shapes of the VKJRF and GRF curves shown in Figures 8c and 8d, provide some visual

evidence for this conclusion). The small differences between accelerations, when multiplied by the relatively small masses of the rigid and wobbling mass tissues, generated correspondingly small forces which, when compared to the GRFs, were not large enough to cause significant differences in the estimated VKJRFs (see Equations [4] - [7]). Since the resultant acceleration of the combined rigid and wobbling mass leg segment was calculated as the weighted average of the two independent accelerations (see Equation [5]), the magnitudes of the rigid and wobbling mass accelerations would have needed to be largely different from one another before the resultant acceleration would have varied enough from the independent rigid mass acceleration, to have caused significant differences in the estimated VKJRFs.

The critically damped response of the body seen in the GRFs following impact (see Figure 8c), is indicative of the natural shock absorption inherent in the human system. Despite having remained very rigid at the knee and ankle joints during landing, the lower extremities of subjects absorbed the applied forces through the heel pad, rigid and wobbling tissues, and joint articulating cartilages of the support leg. In order to further protect and balance themselves after impact, a few subjects almost automatically flexed and then extended their trunks at the hip, upon landing. These rapid displacements of the upper body (trunk

and arms) produced coincidental oscillations in the corresponding GRF curve, at times between impact and the return to body weight. It is suggested that movements such as these were attempts by the subjects to produce a momentary unweighting phase at impact, the result of which would be a reduction in the rate at which the forces were applied.

Although the magnitudes of the peak forces may have been reduced somewhat by these upper body movements, it was not the purpose of this study to achieve the largest PFs possible, but only PFs large enough, and with short enough RTs, to induce independent wobbling mass motion. This was achieved for each subject.

(iii) Vertical Knee Joint Reaction Forces (VKJRF)

Previous investigators (Galea and Norman, 1985), have suggested that joint reaction forces, like the ones calculated in this study, are dramatic underestimations of the actual forces seen by the articulating bone surfaces, and that more accurately, bone-on-bone (BOB) forces, which represent the total of all compressive forces at the joint (including joint reaction forces), should be determined.

For example, BOB forces of magnitude 10 x bw and 24 x bw have been estimated at the ankle joint of ballerinas during a rapid heel to toe movement (Galea and Norman, 1985), and at the knees of subjects landing from a vertical height of just over 1.0 meter (Smith, 1975). These forces far exceed those

knee joint forces calculated in this study. The differences between these measures are due, at least in part, to joint compressions resulting from muscles, tendons and ligaments crossing the joint in tension. As noted previously, the contribution of these tissue components to the total compressive force at a joint can be considerable.

The EMG data of gastrocnemius, biceps femoris, and vastus lateralis, indicated that additional tension across the knee joint was present at impact, due to isometric muscular contractions. In fact, it was this additional tension surrounding and compressing the joint which likely created the stability in the joint (beyond that created by the geometry of the articulating surfaces) necessary for subjects to safely maintain their balance after impact, since the use of joint flexions was discouraged.

Despite the evidence which suggests that there is more to BOB forces than joint reaction forces alone, it was never the intent of this study to determine the total compressive force at the knee. The intent was only to determine the magnitude of the applied force which was transmitted through the segment and across the knee joint, exclusive of all other soft tissues that surround the joint at the articulating surfaces. The development of a more complex model which accounts for BOB forces however, is a project which warrants future consideration.

Model

One of the purposes of this study was to attempt to validate the accuracy of estimated VKJRFs (calculated using both rigid only, and rigid and wobbling link segment models) relative to actual knee joint forces measured directly at the knee joint of the manufactured mechanical model. The strength of the model was in its ability to provide actual VKJRF data, without its performance being questioned as a result of problems associated with accelerometer fixation and high muscle activity, which existed for the subjects.

Ironically, the relative simplicity of the model complicated attempts at creating rigid and wobbling mass accelerations and GRF waveforms with the same characteristics as those exhibited repeatedly by the human system. Numerous pilot experiments were performed prior to final data collection in attempt to determine (manually) the optimal visco-elasticity of the model such that the shapes of the artificially generated waveforms resembled, as closely as possible, those produced by the subjects.

(i) Rigid and Wobbling Mass Accelerations

It became readily apparent that the rigid mass accelerations of the model were similar in shape to those of the subjects, but with much greater IPA magnitudes and shorter durations. The very large initial and second peak magnitudes were attributed to the rigidity of the metal comprising the

rigid mass of the leg. In some cases, the magnitudes of the second peaks were comparable, or even larger than the IPAs. Separate testing with the wobbling mass portion of the leg fastened rigidly to the leg, indicated that the rigidity of the materials used to manufacture the model caused it to vibrate and bounce off the force platform following impact. The introduction of the above knee wobbling mass (bagged rice and bean bags housed in a milk crate and bolted to the thigh plate on the superior surface of the model) proved to partially alleviate the bouncing effect of the model, but not the vibrations.

Regulation of the stiffness and viscosity of the connection between the rigid and wobbling masses, was problematic in several ways. The pin guiding system, which was designed to create some friction damping between the rigid and wobbling masses, allowed for reverberations of the guiding pins in the slot, the result of which was a high frequency vibration (75 Hz) on the wobbling mass accelerations (see Figure 11b). Tightening of the assembly in order to reduce this effect, worked to some extent. It also proved to limit the range and decrease the relative velocity of the vertical translations of the wobbling mass.

The amplitude and duration of the vertical oscillations of the wobbling mass were also regulated by controlling the number and stiffness of the elastic bands

which connected the rigid and wobbling masses. It was found that, within the physical limits of the device, the more elastics used, and the more tightly they were stretched, the more closely the wobbling mass accelerations resembled those of the subjects.

For all combinations of number and stiffness of the elastic bands, the wobbling mass had a tendency, following its initial peak downward displacement, to rebound upwards such that it helped to lift the entire model briefly off the force platform. Although this rebounding effect was not entirely eradicated, it was greatly limited by restricting the vertical displacement of the wobbling mass (by increasing the number and stiffness of the elastics and by increasing the friction in the pin guiding system).

(ii) Vertical Ground Reaction Forces (GRF)

The initial GRF data collected from the model showed dual force peaks to be present just following impact. When released from 10 cm, it was visually apparent that the foot plate was not landing flatly on the force platform, but was striking it on two sides before settling down. As a result, the GRF curves showed two distinct peaks followed by a high frequency vibration. Redistribution of the thigh and trunk wobbling mass, and realignment and levelling of the electromagnet, seemed to eliminate the double foot strike, however, the vibrations following the initial peak persisted

in all cases (see Figure 11c). Visual inspection of the waveform of one trial indicated that the vibration following impact had a frequency of approximately 200 Hz, which approaches the natural frequency of the force platform (260 Hz). It is likely that the model began to vibrate following impact with the force platform, the result of which were corresponding vibrations in the GRFs.

The model was in flight during the unweighting phase of the GRF curve, shown at approximately the 0.2 second mark in Figure 11c. Such undershoots of body weight were typical of the model, and were likely attributable to model rigidity and the inertial rebound of the wobbling mass, as previously discussed. The existence and length of the unweighting phase depended to a large degree, on the relative "loft" of the above knee wobbling mass. As a result of each impact, the above knee wobbling mass became compressed, causing the model to behave more rigidly during future impacts. Regular redistributions of the above knee wobbling mass were required to maintain its loft, and minimize the length of the unweighting phase in the GRFs.

(iii) Vertical Knee Joint Reaction Forces (VKJRF)

In all cases, the estimated VKJRF waveforms of the model had high frequency vibrations on them which were reminiscent of the vibrations present on the corresponding GRF waveforms. The relatively high %RMS errors and especially

poor r values for the VKJRF curves may have been due, in part, to those vibrations. Filtering of the estimated VKJRF data was considered, however, the frequencies of the vibrations on the signals were very similar to the frequencies of the initial force spikes. Any smoothing of the data to eliminate the unwanted vibrations would have likely eliminated the initial peak forces as well.

The peak VKJRFs calculated using rigid mass accelerations only (RRy), were consistently larger than the peak VKJRFs calculated with the wobbling mass accelerations included (RWRy). These differences in VKJRFs reflect the large differences in magnitude between the rigid and wobbling mass accelerations. As discussed earlier, the resultant acceleration of the combined rigid and wobbling mass leg segment is a weighted average of the two independent accelerations. The large differences in accelerations resulted in mean values with magnitudes largely different from the rigid mass accelerations alone. Although an ANOVA was not performed on the model VKJRF results, the estimated knee joint forces were much more accurate and realistic, relative to the actual values (LCRy), when the wobbling mass accelerations were included (RWRy).

Despite these encouraging results, the generalizability of them, to the human system, is questionable. In order to isolate the relative interaction of

two separate tissue components of the human leg, the simplified model was created such that there was a distinctly delineated connection between rigid and non-rigid tissues of the leg. This seemed to eliminate the complications regarding the neural activation of muscle, and the method of accelerometer fixation, which were discussed as possible weaknesses in the method of subject testing. It may be reasonable to say however, that these attempts to design a simplified version of the human system proved only to create an artificial system capable of generating the sought after response, and not necessarily what the human biological response would be under the same conditions.

Considerations For Future Research

It is suggested by the author that, as a result of this study, there seems to be some evidence to suggest that wobbling mass may affect the magnitude of force which is transmitted through the leg segment, and that changes in methodology may be integral to future attempts at quantifying the effect in humans. In particular, the neural activation of the muscular component of the wobbling mass was deemed to be methodologically problematic because of its resultant effect on increasing the muscular rigidity. Similarly, validation of the method of accelerometer fixation used in this study, against other methods, may be necessary if continuation with the outlined experimental protocol is considered.

Due to the perceptions of instability expressed by a few of the subjects, the high muscle activations which were recorded at, and just following impact, were not surprising. Reductions in the degree of activation may be accomplished by changing the method of administration of the applied force. It is suggested that methodologies similar to some of those which have been used successfully in animal research, should be explored on the human scale. For example, Paul et al., (1978) applied forces at various frequencies to the heels of rabbits whose legs were held rigidly in a vertical position by a mechanical jig. With a setup such as this, the magnitudes of the applied forces may be more finely graded, such that the desired result is effected without the administration of unnecessary discomfort to the subject. In addition, the rigidity of the leg is maintained without the conscious muscular effort of the subjects. As a result, the tonic activity of the muscular component of the wobbling mass may be reduced.

Direct validation of the internal joint kinetics of human subjects does not seem likely in the near future of biomechanics research. Indirect attempts at validating VKJRFs of subjects in the future should involve the refinement of the existing mechanical model. Specifically, efforts should be made to more accurately determine the response of the visco-elastic connection between the rigid and wobbling masses of

the model, as it relates to the human system. Given this, it is likely that a more elaborate design of the existing pin guiding system and elastic band assembly (perhaps dashpots and springs), is necessary in order to produce more biologically realistic results. It is also suggested that alternate materials which are less rigid in composition (wood, plastic), and as a result, less likely to vibrate to the same extent as the existing model, might be used in future designs.

SUMMARY AND CONCLUSIONS

In the light of the findings of this study it can be concluded that, for activities such as the one used for subject testing, the estimations of peak VKJRFs, using a combined rigid and wobbling link segment model of the leg, are not significantly different in magnitude relative to those estimations calculated using a rigid mass only link segment model. Apparently, when using the method outlined above, this will always be the case when the magnitudes of the peak rigid and wobbling mass accelerations are similar to each other, as it was found for the subjects in this study. The similarities were reasoned to be a result of high neural activity in the muscular portion of the wobbling mass, and/or the use of an invalid method of accelerometer fixation.

When the neural input to the wobbling mass was eliminated via the manufacture and study of a manufactured model, the rigid mass and wobbling mass accelerations were appreciably different with respect to one another. As a result, estimates of peak VKJRFs were much closer, relative to actual values, when the wobbling mass accelerations were included in the calculations. Peak VKJRFs were greatly overestimated when the rigid mass accelerations alone were used.

Despite the limitations of using the manufactured

model as a method of validation in this study, the model was successful in showing that neural activation was a likely factor contributing to the insignificant subject VKJRF results. In addition, the functional simplicity of the design of the model made it appropriate for this study, whose main purpose was to simplify the resultant motion of the leg such that any wobbling mass effects could be determined easily and at reasonable expense.

It was also suggested that future research in this area should investigate alternate testing protocols which are aimed at limiting the tonic activity of the muscular component of the wobbling mass, while the external forces are being applied. More elaborate methods of creating biologically realistic visco-elastic interfaces between the rigid and wobbling masses of the existing model, may also be necessary for more accurate validations of the human response to impact loading.

BIBLIOGRAPHY

- Blickman, R. The Spring-Mass Model for Running and Hopping. J. Biomechanics, 22(11/12): 1217-1227, 1989.
- Bordelon, R. L. Orthotics, Shoes, and Braces. Orthopedic Clinics of North America, 20(4): 751-757, 1989.
- Brodie, D. A. Techniques of Measurement of Body Composition Part I. Sports Medicine, 5: 11-40, 1988.
- Cavagna, G. A. Elastic Bounce of the Body. J. Appl. Physiol., 29(3): 279-282, 1970.
- Clarys, J. P., and M. J. Marfell-Jones. Anthropometric Prediction of Component Tissue Masses in the Minor Limb Segments of the Human Body. Human Biology, 58(5): 761-769, 1986a.
- Clarys, J. P., and M. J. Marfell-Jones. Anatomical Segmentation in Humans and the Prediction of Segmental Masses from Intra-segmental Anthropometry. Human Biology, 58(5): 771-782, 1986b.
- Clarys, J. P., A. D. Martin, and D. T. Drinkwater. Gross Tissue Weights in the Human Body By Cadaver Dissection. Human Biology, 56(3): 459-473, 1984.
- Dempster, W. T., and G. R. L. Gaughran. Properties of Body Segments Based on Size and Weight. Am. J. Anatomy, 120: 33-54, 1967.
- Galea, V., and R. W. Norman. Bone-on-Bone Forces at the Ankle Joint During a Rapid Dynamic Movement. In: Biomechanics IX-A (eds. D. A. Winter, R. W. Norman, R. P. Wells, K. C. Hayes, and A. E. Patla), 71-76, 1985.

- Galea, V., S. Ormerod, N. White, J. D. MacDougall, and C. E. Webber. Body Composition by Photon Absorptiometry. Can. J. Sport Sciences, 15(2): 143-148, 1990.
- Gilbert, J. A., M. G. Maxwell, J. H. McElhaney, and F. W. Clippinger. A System to Measure the Forces and Moments at the Knee and Hip During Level Walking. J. Orth. Res., 2: 281-288, 1984.
- Gruber, K., J. Denoth, E. Stuessi, and H. Ruder. The Wobbling Mass Model. In: Biomechanics X-B (ed. B. Jonsson), 1095-1099, 1987.
- Hatze, H. A New Method For the Simultaneous Measurement of the Moment of Inertia, the Damping Coefficient and the Location of the Center of Mass of a Body Segment in situ. Eur. J. Appl. Physiol., 34: 217-226, 1975.
- Hennig, E. M., and M. A. Lafortune. Tibial Bone and Skin Accelerations During Running. In C. E. Cotton, M. Lamontagne, D. G. E. Robertson, and J. P. Stothart (Eds.), Proceedings of the Vth Biannual Conference of the Canadian Society for Biomechanics, Ottawa: Spodym. Publ., 1988.
- Hennig, E. M., and M. A. Lafortune. Relationships Between Ground Reaction Force and Tibial Bone Acceleration Parameters. Int. J. Sport Biomechanics, 7: 303-309, 1991.
- Lafortune, M. A., and E. M. Hennig. Contribution of Angular Motion and Gravity to Tibial Acceleration. Med. and Sci. in Sports and Exercise, 23(3): 360-363, 1991.
- Lees, A. Methods of Impact Absorption When Landing From a Jump. Medicine in Engineering, 10(4): 207-211, 1981.
- Light, L. H., and G. E. McLellan. Skeletal Transients Associated With Heel Strike. J. Physiology, 272: 9-10P, 1977.

- Light, L. H., G. E. McLellan, and L. Klenerman. Skeletal Transients on Heel Strike in Normal Walking With Different Footwear. J. Biomechanics, 13: 477-480, 1980.
- Lukaski, H. C. Methods For the Assessment of Human Body Composition: Traditional and New. Am. J. Clinical Nutrition, 46: 537-556, 1987.
- McGill, S. M., A. Thorstensson, and R. W. Norman. Non-rigid Response of the Trunk to Dynamic Axial Loading: An Evaluation of Current Modelling Assumptions. Clinical Biomechanics, 4: 45-50, 1989.
- Mizrahi, J., and Z. Susak. Analysis of Parameters Affecting Impact Force Attenuation During Landing in Human Vertical Free Fall. Medicine in Engineering, 11(3): 141-147, 1982a.
- Mizrahi, J., and Z. Susak. In-vivo Elastic and Damping Response of the Human Leg to Impact Forces. J. Biomechanical Engineering, 104: 63-65, 1982b.
- Morris, J. R. W. Accelerometry - A Technique For the Measurement of Human Body Movements. J. Biomechanics, 6: 729-736, 1973.
- Morrison, J. B. The Mechanics of the Knee Joint in Relation to Normal Walking. J. Biomechanics, 3: 51-61, 1970.
- Nigg, B. M., W. Herzog, and L. J. Read. Effect of Viscoelastic Shoe Insoles on Vertical Forces in Heel-toe Running. Am. J. Sports Medicine, 16(1): 70-76, 1988.
- Özgüven, H., and N. Berme. An Experimental and Analytical Study of Impact Forces During Human Jumping. J. Biomechanics, 21(2): 1061-1066, 1988.

- Paul, I. L., M. B. Munro, P. J. Abernethy, S. R. Simon, E. L. Radin, and R. M. Rose. Musculo-Skeletal Shock Absorption: Relative Contribution of Bone and Soft Tissues at Various Frequencies. J. Biomechanics, 11: 237-239, 1978.
- Radin, E. L., R. B. Orr, J. L. Kelman, I. L. Paul, and R. M. Ross. Effect of Prolonged Walking on Concrete on the Knees of Sheep. J. Biomechanics, 15: 487-492, 1982.
- Radin, E. L., H. G. Parker, J. W. Pugh, R. S. Steinberg, I. L. Paul, and R. M. Rose. Response of Joints to Impact Loading - III. Relationship Between Trabecular Microfractures and Cartilage Degeneration. J. Biomechanics, 6: 51-57, 1973.
- Rome, K. Behaviour of Orthotic Materials in Chiropody. Am. J. Pod. Med. Assoc., 80(9): 471-478, 1990.
- Rome, K. A Study of the Properties of Materials Used in Podiatry. Am. J. Pod. Med. Assoc., 81(2): 73-83, 1991.
- Roseau, M. Vibrations in Mechanical Systems: Analytical Methods and Applications. Springer-Verlag Publishers, Berlin; Heidelberg, 1987.
- Salathé, E. P., G. A. Arangio, and E. P. Salathé. The Foot as a Shock Absorber. J. Biomechanics, 23(7): 655-659, 1990.
- Sanders, R. H., B. D. Wilson, and R. K. Jenson. Accuracy of Derived Ground Reaction Force Curves for a Rigid Link Human Body Model. Int. J. Sport Biomechanics, 7: 330-343, 1991.
- Scott, S. H., and D. A. Winter. Internal Forces at Chronic Running Injury Sites. Med. and Sci. in Sports and Exercise, 22(3): 357-369, 1990.

- Simon, S. R., E. L. Radin, and I. L. Paul. The Response of Joints to Impact Loading - II. In vivo Behaviour of Subchondral Bone. J. Biomechanics, 5: 267-272, 1972.
- Smith, A. J. Estimates of Muscle and Joint Forces at the Knee and Ankle During a Jumping Activity. J. Human Movement Studies, 1: 78-86, 1975.
- Voloshin, A., and J. Wosk. Influence of Artificial Shock Absorbers on Human Gait. Clin. Orthopaedics, 160: 52-56, 1981.
- Voloshin, A., and J. Wosk. An In Vivo Study of Low Back Pain and Shock Absorption in the Human Locomotor System. J. Biomechanics, 15(1); 21-27, 1982.
- Walshaw, A. C. Mechanical Vibrations With Applications. Ellis Horwood Limited, England, 1984.
- Willemsen, A. Th. M., T. A. van Alsté, and H. B. K. Boom. Real-time Gait Assessment Utilizing a New Way of Accelerometry. J. Biomechanics, 23(8): 859-863, 1990.
- Ziegert, J. C., and J. L. Lewis. The Effect of Soft Tissue on Measurements of Vibrational Bone Motion by Skin-mounted Accelerometers. ASME J. Biomechanical Eng., 101: 218-220, 1979.

APPENDIX I - Nomenclature

A/D	- Analog to Digital
BOB	- Bone-On-Bone forces
bw	- Body Weight
c	- coefficient of damping
CMRR	- Common Mode Rejection Ratio
DPA	- Dual Photon Absorptiometry
EMG	- Electromyography
g	- acceleration due to gravity (9.81 m/s^2)
G	- the Gastrocnemius muscle
GRF	- Ground Reaction Force
H	- a Hamstring muscle (biceps femoris)
IPA	- Initial Peak Acceleration
k	- spring stiffness
LCRY	- actual vertical knee joint reaction force of the model (from the Load Cell)
MRI	- Magnetic Resonance Imaging
MVC	- Maximum Voluntary Contraction
PAT	- Time of Peak muscle Activity
PF	- Peak Force
RRY	- estimated vertical knee joint force calculated using only a rigid mass link segment model of the leg
RT	- Rise Time (time to Peak Force)
RWRY	- estimated vertical knee joint force calculated using a rigid and wobbling mass link segment model of the leg
SD	- Standard Deviation
TA	- the Tibialis Anterior muscle
VL	- the Vastus Lateralis muscle (quadriceps)
VKJRF	- Vertical Knee Joint Reaction Force
y	- linear displacement
\dot{y}	- linear velocity
\ddot{y}	- linear acceleration